Divergent Evolutionary Rates of Primate Brain Regions as Revealed by Genomics and Transcriptomics

Xiao-Lin Zhuang[1,2], Yong Shao [1,2], Chun-Yan Chen[3], Long Zhou[4,5], Yong-Gang Yao [1,2,6,7,8], David N. Cooper[9], Guo-Jie Zhang[4,5], Wen Wang[1,3], and Dong-Dong Wu [1,7,8,*]

[1]Key Laboratory of Genetic Evolution & Animal Models, Kunming Natural History Museum of Zoology, Kunming Institute of Zoology, Chinese Academy of Sciences, Kunming 650201, China

[2]Kunming College of Life Science, University of the Chinese Academy of Sciences, Kunming 650204, China

[3]School of Ecology and Environment, Northwestern Polytechnical University, Xi'an 710072, China

[4]Center of Evolutionary & Organismal Biology, and Women's Hospital at Zhejiang University School of Medicine, Zhejiang University, Hangzhou 310000, China

[5]Liangzhu Laboratory, Zhejiang University Medical Center, Hangzhou 310000, China

[6]Key Laboratory of Animal Models and Human Disease Mechanisms of Chinese Academy of Sciences & Yunnan Province, Kunming Institute of Zoology, Chinese Academy of Sciences, Kunming, Yunnan 650201, China

[7]National Resource Center for Non-Human Primates, Kunming Primate Research Center, and National Research Facility for Phenotypic & Genetic Analysis of Model Animals (Primate Facility), Kunming Institute of Zoology, Chinese Academy of Sciences, Kunming, Yunnan 650107, China

[8]KIZ-CUHK Joint Laboratory of Bioresources and Molecular Research in Common Diseases, Kunming Institute of Zoology, Chinese Academy of Sciences, Kunming, Yunnan 650201, China

[9]Institute of Medical Genetics, School of Medicine, Cardiff University, Cardiff CF14 4XN, UK

*Corresponding author: E-mail: wudongdong@mail.kiz.ac.cn.

Accepted: January 30, 2024

Abstract

Although the primate brain contains numerous functionally distinct structures that have experienced diverse genetic changes during the course of evolution and development, these changes remain to be explored in detail. Here we utilize two classic metrics from evolutionary biology, the evolutionary rate index (ERI) and the transcriptome age index (TAI), to investigate the evolutionary alterations that have occurred in each area and developmental stage of the primate brain. We observed a higher evolutionary rate for those genes expressed in the non-cortical areas during primate evolution, particularly in human, with the highest rate of evolution being exhibited at brain developmental stages between late infancy and early childhood. Further, the transcriptome age of the non-cortical areas was lower than that of the cerebral cortex, with the youngest age apparent at brain developmental stages between late infancy and early childhood. Our exploration of the evolutionary patterns manifest in each brain area and developmental stage provides important reference points for further research into primate brain evolution.

Key words: primate, brain, development, evolution, evolutionary rate, transcriptome age.

Significance

Our understanding of how various brain regions, particularly non-cortical areas, evolve in primates is incomplete and requires thorough exploration. We performed a comprehensive investigation into the unique evolutionary patterns of each primate brain region, uncovering previously unnoticed evolutionary patterns and identifying potential genetic foundations for primate brain evolution.

Introduction

Primates, especially humans, are remarkable for their brains, behaviors, and cognitive abilities, unique attributes that have been acquired over an extended period of evolutionary time. Over the last decade, and benefiting from rapid advances in comparative genomics, transcriptomics and epigenomics, studies across primate species have generated many new and fundamental insights into the genetic underpinnings of primate brain evolution (Gilad et al. 2006; Lui et al. 2011; Bernard et al. 2012; Dehay et al. 2015; Bakken et al. 2016; He et al. 2017; Amiri et al. 2018; Kronenberg et al. 2018; Kanton et al. 2019; Agoglia et al. 2021). However, most studies have focused either on the whole brain or the neocortex. Precisely how each specific brain region, and in particular the non-cortical areas, have evolved is not fully understood and remains to be explored in detail. It is therefore very important to acquire a comprehensive understanding of the evolutionary patterns experienced by each individual brain region.

The primate brain comprises a number of functionally distinct structures, the human brain being the most elaborate; different brain structures vary dramatically both within and between primate lineages, reflecting the functional specialization of the brain over evolutionary time (Sousa et al. 2017a; DeCasien and Higham, 2019). There is now abundant molecular genetic evidence to support the notion of functional specialization of the primate brain; for example, in terms of gene expression, different human brain structures exhibit diverse levels of expression with respect to the same groups of genes, and each brain structure has its own uniquely specific gene markers (Hawrylycz et al. 2012; Bhaduri et al. 2021).

Further, previous studies of the entire primate brain have supported the contention that genes involved in brain function evolved more rapidly in primates than in rodents (Dorus et al. 2004), particularly those genes linked to brain development (Dorus et al. 2004). This is reflected in a positive correlation between the ratio of non-synonymous to synonymous mutations of genes and primate brain evolution. Moreover, gene age, namely the estimated time since the emergence of the gene according to phylogenetic analyses, could reflect the evolutionary trajectory of the primate brain (Domazet-Loso and Tautz, 2010). Here, based on previous research (Domazet-Loso et al. 2007; Domazet-Loso and Tautz, 2010; Quint et al. 2012), we leveraged genome sequence data from the Primate Genome Project, which integrated 50 primate genomes sequenced in our laboratory (Shao et al. 2023), utilizing two classic indices—the evolutionary rate index (ERI) and the transcriptome age index (TAI)—to fully investigate the evolution of each brain area in eight major primate ancestral lineages leading to human. Our study not only reveals novel and hitherto underappreciated evolutionary patterns associated with specific primate brain areas but also, and more broadly, identifies the potential genetic underpinnings of primate brain evolution and development.

Results

Diverse Evolutionary Rates of Different Brain Areas During Primate Evolution

The functional specialization of primate brain areas implies that different areas might be subject to differing levels of natural selection. This raises basic questions as to which primate brain areas have evolved at a high rate, and which have been relatively conserved over evolutionary time (Lui et al. 2011; Dehay et al. 2015; Sousa et al. 2017b). To address these questions, we deeply investigated the evolutionary rates of various brain regions in primates by integrating massive transcriptome data and selection signals at the gene sequence level. To explore the evolutionary rates, we derived the evolutionary rate index (ERI) by means of the formula $ERI = \sum[(dN/dS) * E]/\sum E$ (detailed in Materials and Methods), which was referred to previously (Quint et al. 2012).

Employing Primate Genome Project data (Shao et al. 2023), we generated dN/dS (ratio of non-synonymous to synonymous substitutions) values of primate orthologous genes from large scale comparative genomics analyses to reveal the evolutionary genetic patterns exhibited by different brain areas and/or during specific developmental stages. Then, we combined gene expression data from 45 rhesus macaque brain regions (Li et al. 2019) with the dN/dS values of genes from eight major primate ancestral lineages leading to human speciation to generate a measure of the evolutionary rate of each brain area in each primate lineage (Fig. 1A and B, supplementary table S1, Supplementary Material online). Unexpectedly, and contrary to received opinion that contends it was the neocortex which experienced the most rapid evolution in primates (Lui

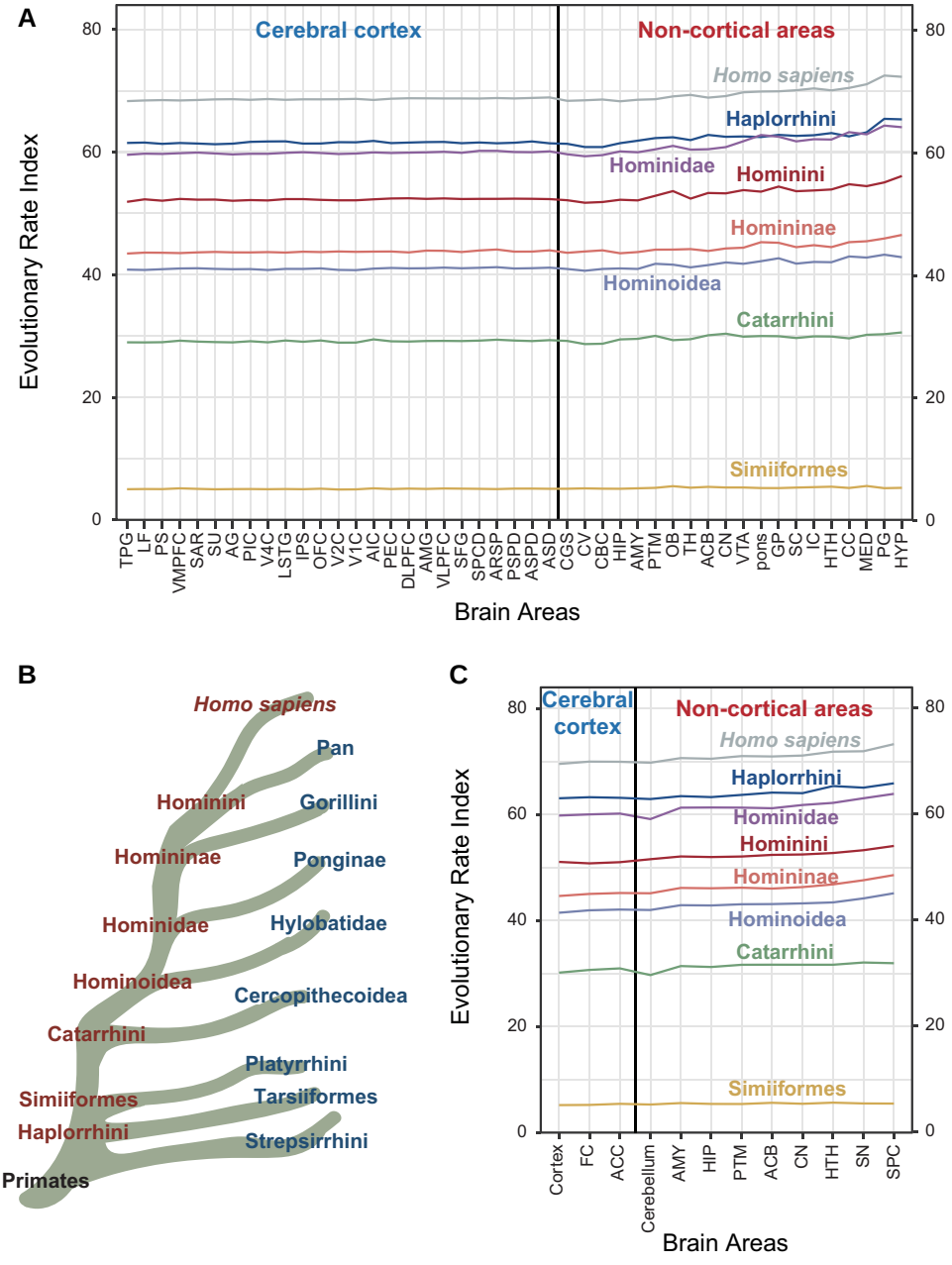

Fig. 1.—Evolutionary patterns of different brain areas in different primate lineages. (A) Evolutionary rate index of 45 brain areas in different primate lineages based on gene expression data of rhesus macaque brain (Li et al. 2019). The terms ascribed to the brain areas are given below and in supplementary table S1, Supplementary Material online. (B) Simplified diagram of the phylogenies of the different primate lineages. (C) Evolutionary rate index of 12 brain areas in different primate lineages based on human brain gene expression data derived from the Genotype-Tissue Expression (GTEx) project, release V8. The terms ascribed to the various brain areas are given below and in supplementary table S2, Supplementary Material online. CN, caudate nucleus; PTM, putamen; GP, globus pallidus; AMY, amygdala; HIP, hippocampus; CGS, cingulate sulcus; TH, thalamus; HTH, hypothalamus; SC, superior colliculus; IC, inferior colliculus; pons, Pons; CV, cerebellar vermis; HYP, hypophysis; ACB, accumbens nucleus; CC, corpus callosum; VTA, ventral tegmental area; OB, olfactory bulb; MED, medulla; PG, pineal gland; SU, superior postcentral dimple; IPS, intraparietal sulcus; LF, lateral fissure; PEC, parietal area; AMG, anterior marginal gyrus; AG, angular gyrus; LSTG, lateral superior temporal gyrus; TPG, temporal polar gyrus; DLPFC, dorsolateral prefrontal cortex; VLPFC, ventral lateral prefrontal cortex; ASPD, anterior supraprincipal dimple; V1C, primary visual cortex; V2C, visual cortex V2; V4C, visual cortex V4; SFG, superior frontal gyrus; CBC, cerebellar cortex; VMPFC, ventromedial prefrontal cortex; AIC, anterior insula cortex; PIC, posterior insula cortex; OFC, orbitofrontal cortex; PSPD, posterior supraprincipal dimple; SAR, superior arcuate sulcus; PS, principal sulcus; ASD, anterior subcentral dimple; ARSP, arcuate sulcus spur; SPCD, superior precentral dimple; FC, frontal cortex; ACC, anterior cingulate cortex; SN, substantia nigra; SPC, spinal cord.

Table 1
t-Test results of ERI values between non-cortical regions and cortical regions, based on rhesus macaque brain expression data (Li et al. 2019)

Lineages	*P* values
Homo sapiens	0.0005718
Hominini	0.0001137
Homininae	0.0001537
Hominidae	8.10E−05
Hominoidea	3.21E−05
Catarrhini	1.57E−05
Simiiformes	5.40E−07
Haplorrhini	0.000523

Table 2
t-Test results of ERI values between non-cortical regions and cortical regions, based on human brain expression data (Zhu et al. 2018)

Lineages	*P* values
Homo sapiens	0.001676
Hominini	0.000102
Homininae	0.000831
Hominidae	0.002613
Hominoidea	0.000853
Catarrhini	0.02084
Simiiformes	0.04544
Haplorrhini	0.007484

et al. 2011; Dehay et al. 2015), we found that many non-cortical areas, such as the hypophysis (HYP), pineal gland (PG), and medulla (MED), displayed significantly higher evolutionary rates compared to areas of the cerebral cortex (Fig. 1A, Table 1, supplementary table S1, Supplementary Material online); these non-cortical areas are key endocrine glands with the potential to influence individual development, cognitive ability and circadian rhythm (Lovick and Li, 1989; Phansuwan-Pujito et al. 1999; Sapede and Cau, 2013; Alatzoglou et al. 2020; Patel et al. 2020). Moreover, the corpus callosum (CC), hypothalamus (HTH), inferior colliculus (IC), and superior colliculus (SC) also displayed significantly higher evolutionary rates than cerebral cortex (Fig. 1A, Table 1, supplementary table S1, Supplementary Material online); these non-cortical areas are essential for the coordination of activities between the two cerebral hemispheres and for the regulation of both visceral and endocrine activity, as well as the auditory and visual senses (Buckingham, 1977; Wurtz and Albano, 1980; Paul et al. 2007; Trachtman, 2010; Pickles, 2015; Blaauw and Meiners, 2020). Furthermore, combining gene expression data derived from 12 human brain areas from the GTEx project (release V8) (GTEx Consortium, 2020) with the dN/dS values of genes in eight major primate ancestral lineages leading to human speciation as a means to measure the evolutionary rate of each brain area, also yielded similar findings (Fig. 1C, Table 2, supplementary table S2, Supplementary Material online). Notably, *Homo sapiens* and the Haplorrhini lineages exhibited higher evolutionary rates than other primate lineages, suggestive of the rapid evolution of brain areas in these two lineages (Fig. 1A and C, supplementary tables S1 and S2, Supplementary Material online).

Furthermore, to exclude the effect of a strong negative correlation between dN/dS values and transcriptional abundance on the calculation of ERI values, we performed Pearson correlation analyses (Fig. 2A and B). The results showed that, whether they were based on rhesus macaque brain expression profiles (Fig. 2A) or human brain expression profiles (Fig. 2B), the negative correlations between the dN/dS values and transcriptional abundance were weak (−0.1102 to −0.0263), indicating that both dN/dS values and transcriptional abundance could be regarded as complementary measures. In particular, there were only a few differences in the negative correlation coefficients between the cortical areas and non-cortical areas (Fig. 2A and B), indicating that the conclusion that non-cortical areas evolved faster than cortical areas was reliable.

Since there were many types of cell in different brain regions, it is necessary to further explore the roles of cell type differences in reconstructing the evolutionary rates. Thus, we utilized the single cell RNA-seq data from six brain regions (including cerebellum, mediodorsal thalamic nucleus, striatum, amygdala, hippocampus, and dorsolateral prefrontal cortex) of two E110 (embryonic day 110) rhesus macaque brains from previously published research (Zhu et al. 2018), combined with dN/dS values from eight major primate ancestral lineages leading to human speciation, to calculate the ERI values of each cell type from each brain region in each primate ancestral node (Fig. 3). The results indicated that many cell types in non-cortical areas displayed higher evolutionary rates compared to that in the dorsolateral prefrontal cortex, especially the microglial cells (Fig. 3). Since microglia are critically involved in many physiological and pathological brain processes, including neurodegeneration (Geirsdottir et al. 2020), the rapid evolution of microglia may suggest their key role in primate brain evolution. These results strongly supported the conclusion that non-cortical areas evolved faster than cortical areas.

The rapid evolution of protein-coding genes related to the primate non-cortical areas including limbic system implies that brain functions related to emotional expression and social cognition have played vital roles during primate evolution. This finding contrasts with the traditional view that the neural basis of emotional behavior has been evolutionarily conserved but is consistent with a previous comparative anatomy study which reported evolutionary specializations of the human limbic system (Barger et al. 2014). Meanwhile, a previous study has also reported that genes expressed in the cortical regions of the brain exhibited lower evolutionary rates than genes expressed in

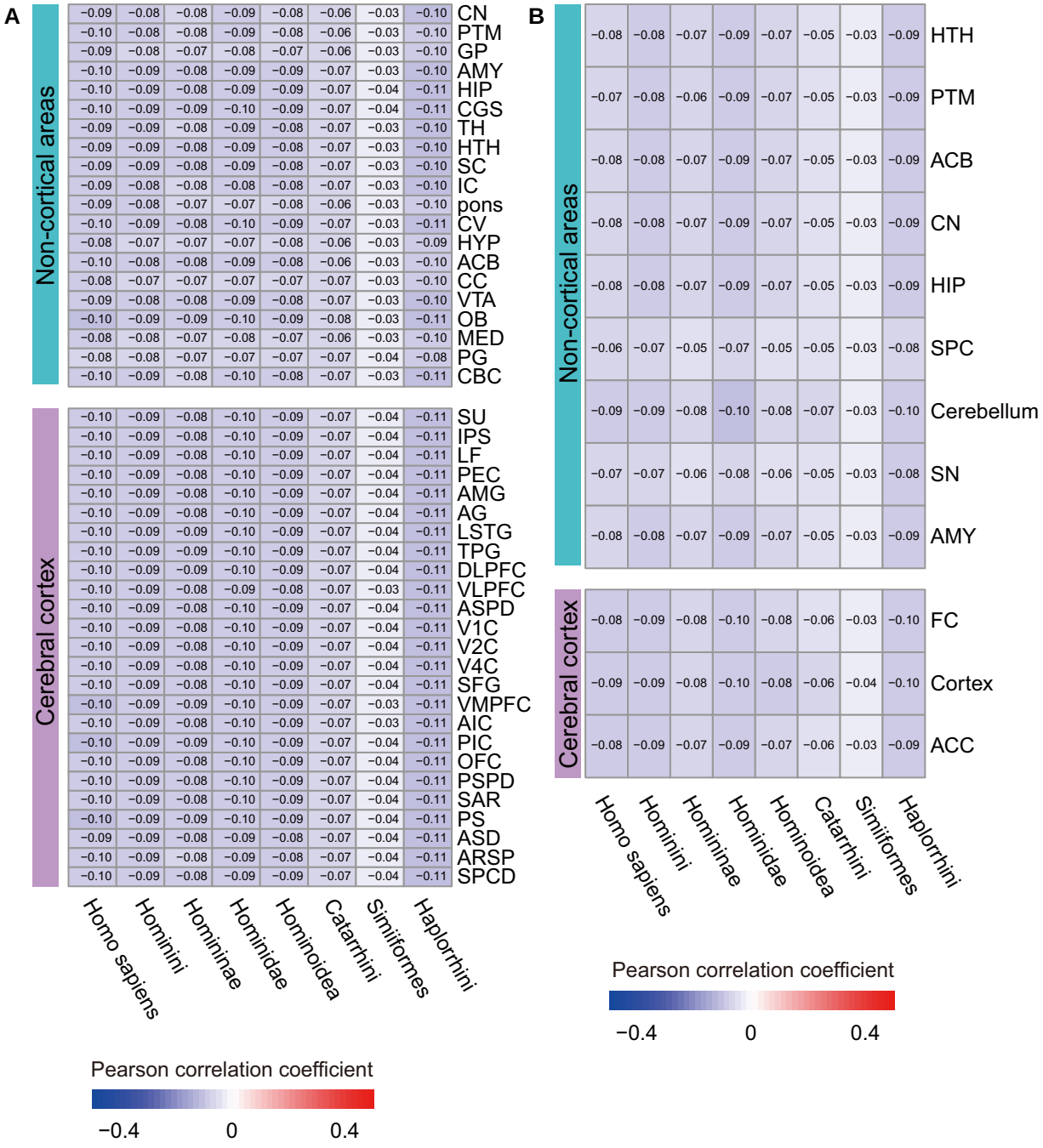

Fig. 2.—Pearson correlation analyses of different brain areas in different primate lineages. Heatmap displaying the Pearson correlation coefficient between dN/dS in each primate ancestral node and transcriptional abundance in each brain tissue, based on rhesus macaque brain data (A) (Li et al. 2019) and based on the human brain data (B), respectively. Cortical and non-cortical areas are shown separately. The specific Pearson correlation coefficients are shown in the figure. CN, caudate nucleus; PTM, putamen; GP, globus pallidus; AMY, amygdala; HIP, hippocampus; CGS, cingulate sulcus; TH, thalamus; HTH, hypothalamus; SC, superior colliculus; IC, inferior colliculus; pons, Pons; CV, cerebellar vermis; HYP, hypophysis; ACB, accumbens nucleus; CC, corpus callosum; VTA, ventral tegmental area; OB, olfactory bulb; MED, medulla; PG, pineal gland; SU, superior postcentral dimple; IPS, intraparietal sulcus; LF, lateral fissure; PEC, parietal area; AMG, anterior marginal gyrus; AG, angular gyrus; LSTG, lateral superior temporal gyrus; TPG, temporal polar gyrus; DLPFC, dorsolateral prefrontal cortex; VLPFC, ventral lateral prefrontal cortex; ASPD, anterior supraprincipal dimple; V1C, primary visual cortex; V2C, visual cortex V2; V4C, visual cortex V4; SFG, superior frontal gyrus; CBC, cerebellar cortex; VMPFC, ventromedial prefrontal cortex; AIC, anterior insula cortex; PIC, posterior insula cortex; OFC, orbitofrontal cortex; PSPD, posterior supraprincipal dimple; SAR, superior arcuate sulcus; PS, principal sulcus; ASD, anterior subcentral dimple; ARSP, arcuate sulcus spur; SPCD, superior precentral dimple; SPC, spinal cord; SN, substantia nigra; FC, frontal cortex; ACC, anterior cingulate cortex.

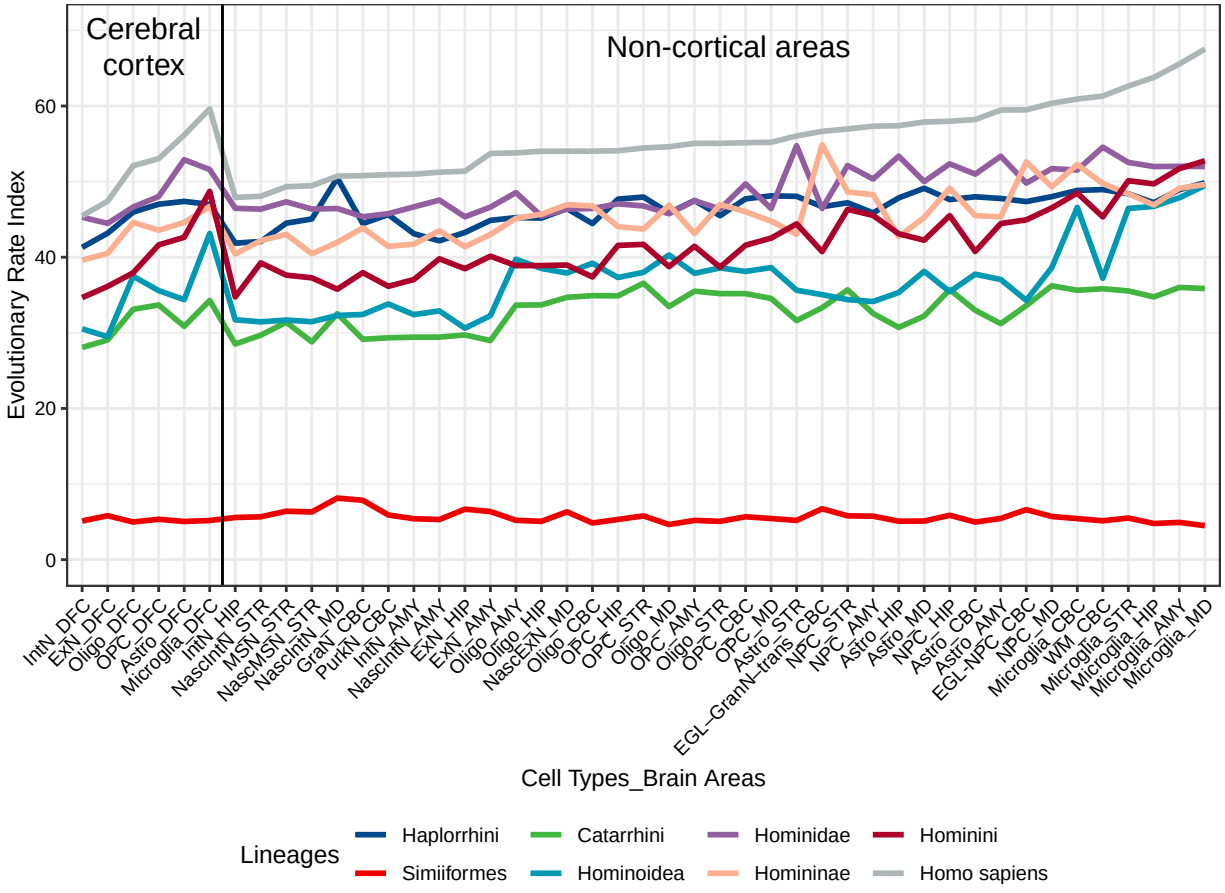

Fig. 3.—Evolutionary patterns of different cell types of various brain areas in different primate lineages. Evolutionary rate index of 16 cell types of 6 brain areas in different primate lineages based on single cell RNA-seq data of rhesus macaque embryonic brains (Zhu et al. 2018). The terms ascribed to the brain areas are given below. DFC, dorsolateral prefrontal cortex; HIP, hippocampus; AMY, amygdala; STR, striatum; MD, mediodorsal thalamic nucleus; CBC, cerebellum; ExN, excitatory neuron; InN, inhibitory neuron; Astro, astrocyte; OPC, oligodendrocyte progenitor cell; Oligo, oligodendrocyte; NPC, neuronal progenitor cell; NascInN, nascent inhibitory neuron; NascMSN, nascent medium spiny neuron; MSN, medium spiny neuron; NascExN, nascent excitatory neuron; EGL-NPC, external granular layer neuronal progenitor cell; WM-NPC, white matter neuronal progenitor cell; EGL-GraN-trans, external granular layer transition to granule neuron; GraN, granule neuron; PurkN, Purkinje neuron.

the non-cortical regions (Tuller et al. 2008), a finding which concurred with our conclusions about the evolutionary patterns.

Rapid Evolution of Primate Brain Development in Early Childhood

We further explored whether different brain regions at different developmental stages in various primate lineages might also display diverse evolutionary rates. To this end, we leveraged a total of 577 human brain development transcriptomes from six brain areas, namely cerebellar cortex, mediodorsal nucleus of the thalamus, striatum, amygdala, hippocampus, and neocortex, and covering a range of developmental stages (Zhu et al. 2018), to measure the evolutionary rate of each area in each primate lineage during development (Fig. 4A and B, supplementary table S4, Supplementary Material online).

Five of the six brain areas (the exception being cerebellar cortex) exhibited a similar mountain-like pattern in terms of their evolutionary rates viewed across developmental stages (Fig. 4A). In the amygdala (AMY), hippocampus (HIP), neocortex (NCX), and mediodorsal nucleus of the thalamus (MD), the evolutionary rate trajectory showed a trend to increase from stage w5 (35 pcw [post-conception weeks] to 0.3 py [post-natal years]) to w6 (0.5 py to 2.5 py) (Fig. 4A and B); this stage was also defined as late fetal to early childhood, after which the trajectory flattened out or even declined. In the striatum (STR), the evolutionary rate reached the peak from stage w6 to w7 (2.8 py to 10.7 py) (Fig. 4A and B), which was also defined as childhood. However, in the cerebellar cortex (CBC), the trajectory showed different developmental trends in different primate ancestral nodes (Fig. 4A and B); the evolutionary rate in the Haplorrhini and Hominidae lineages reached its peak from stage w7 to w8 (13 py to 19 py), that was

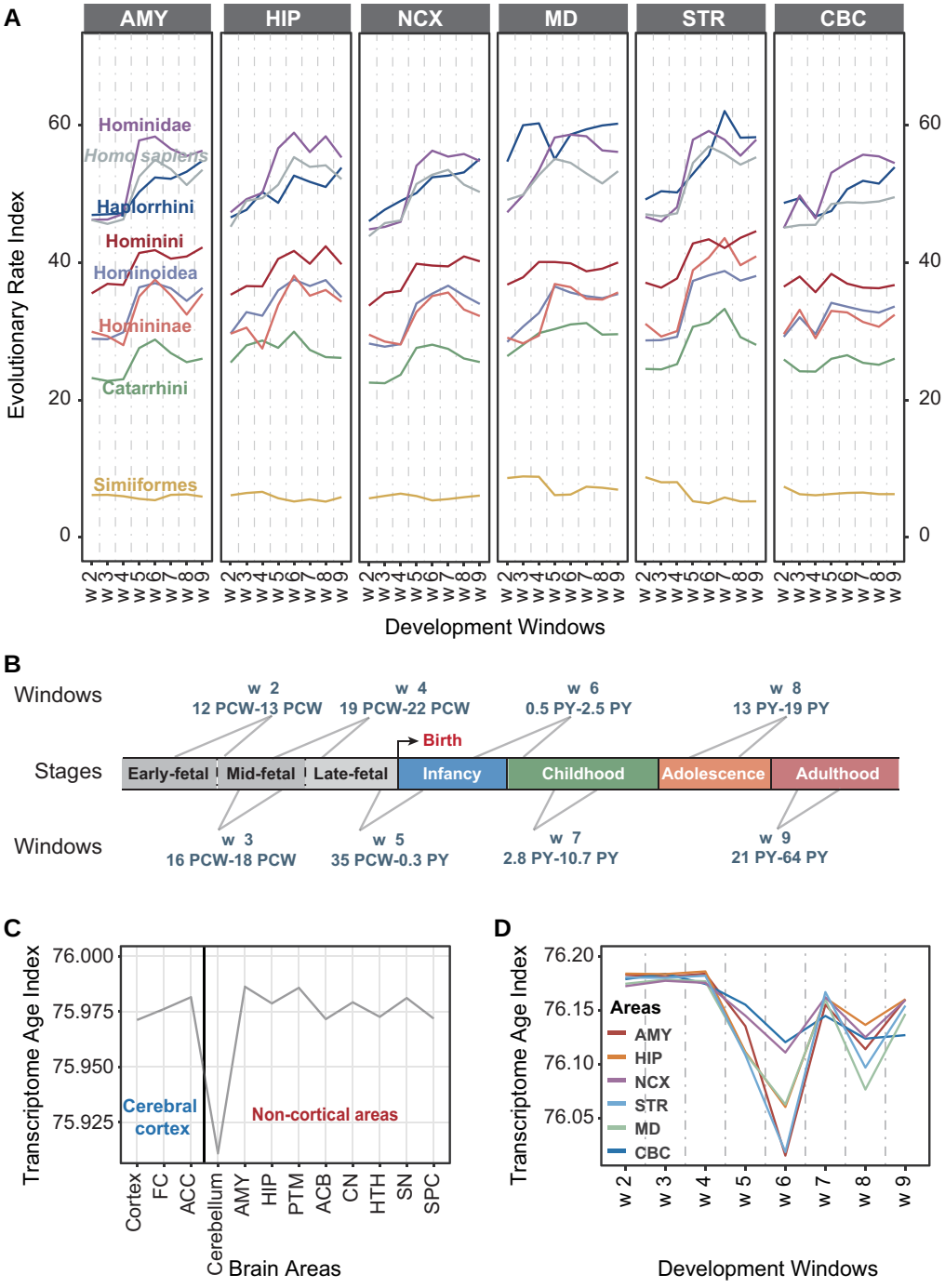

Fig. 4.—Evolutionary patterns of different developmental stages in different primate lineages and the transcriptome age of different human brain areas in diverse developmental stages. (A) Evolutionary rate index of amygdala (AMY), hippocampus (HIP), neocortex (NCX), mediodorsal nucleus of thalamus (MD), striatum (STR), and cerebellar cortex (CBC) during the course of brain development in different primate lineages based on gene expression data from the developing human brain (Zhu et al. 2018). The division of the developmental windows is as in panel B. (B) The developmental stage spans of the samples used in our research; above and below are the specific developmental time spans of the samples included in each developmental window, referenced from Zhu et al. (2018) and Li et al. (2019). (C) Transcriptome age index of 12 brain areas in human, human brain transcriptomes derived from Aguet et al.; the terms ascribed to the different brain areas are the same as those in Fig. 1C. (D) Transcriptome age index of human amygdala (AMY), neocortex (NCX), hippocampus (HIP), striatum (STR), mediodorsal nucleus of the thalamus (MD), and cerebellar cortex (CBC) in different developmental stages, human brain development transcriptomes were derived from Zhu et al. (2018). The division of the developmental windows was as in panel B.

also defined as adolescence, whereas the evolutionary rate in other primate lineages reached its peak from stage w5 to w6. The above results suggested that all brain regions in primates evolved rapidly after birth, and reached their peaks during infancy, childhood, or adolescence (Fig. 4A and B).

The development of primate brain is a long drawn out process that continues well into adulthood. Previous research has shown that early childhood, especially the period between term birth and ∼2 yr of age, is crucial for human brain development and for the establishment of cognitive abilities and behaviors, as well as for influencing the subsequent risk of neuropsychiatric disorders such as autism and schizophrenia (Gilmore et al. 2018). Further, previous research has also indicated that brain development during childhood and adolescence is essential for the maturity of advanced cognitive and behavioral abilities in primates (Pelletier and Neuman, 2014; Vijayakumar et al. 2018). Therefore, the different evolutionary rate trajectories of different brain regions in different primate ancestral nodes have suggested imbalances in primate brain evolution, and these evolutionary patterns may be related to the evolution of specific brain phenotypes in different primate ancestors.

Our findings are consistent with the view that the primate brain has evolved rapidly over the developmental period 0.5 py to 2.5 py (i.e. late infancy to early childhood) (Zhu et al. 2018), which probably accounts for much of the rapid evolution experienced by primates, particularly in the lineages leading to human.

Varied Transcriptome Ages of Different Human Brain Regions During Development

Based on comparative genome analyses of metazoan genome sequences, a crucial finding has been that a large number of genes have arisen anew during the evolution of the respective lineages (Force et al. 1999; Domazet-Loso and Tautz, 2003; Long et al. 2003; Choi and Kim, 2006). The emergence of these novel genes has contributed greatly to phenotypic evolution, and has also been important for primate brain evolution (Chen et al. 2013).

It is possible to trace evolutionary innovations by calculating transcriptome ages for different human brain areas during development by employing a combination of genome and transcriptome data (Domazet-Loso et al. 2007; Domazet-Loso and Tautz, 2010). Here, relying on the large number of primate genomes recently made available through the Primate Genome Project (Shao et al. 2023), we were able for the first time to ascertain the evolutionary gene age (i.e. the estimated time since the emergence of the gene according to phylogenetic analyses) of human protein-coding genes based on a previous pipeline (Zhang et al. 2011; Shao et al. 2019). The expression data for human protein-coding genes were obtained from previously published work (Zhu et al. 2018; GTEx Consortium 2020). We then applied the genomic phylostratigraphy principle (Domazet-Loso et al. 2007; Domazet-Loso and Tautz, 2010) to calculate the transcriptome age index (TAI) of different human brain areas and different developmental stages to measure the transcriptome age by means of the formula $TAI = \sum(A * E)/\sum E$ (detailed in Materials and Methods, Fig. 4C and D, supplementary tables S5 and S6, Supplementary Material online).

We found that the non-cortical areas, especially the cerebellum, tend to exhibit low transcriptome age values and to have accumulated more evolutionarily young genes as compared with the cerebral cortex (Fig. 4C, supplementary table S5, Supplementary Material online), concurring with our above finding that the non-cortical areas evolved more rapidly than the cerebral cortex. Furthermore, consistent with our aforementioned observation on the evolutionary rate trajectory during development, we found that transcriptome age values also displayed a tendency to decrease from developmental stage 0.5 py to 2.5 py (Fig. 4B and D, supplementary table S6, Supplementary Material online). These findings corroborated our earlier conclusion, based on evolutionary rate values, that the stage of development from 0.5 py to 2.5 py evolved particularly rapidly in the lineages leading to human (Fig. 4A, B, and D).

Discussion

Primate brain evolution has been characterized by a series of distinct genetic changes impacting different brain areas in different primate lineages. It was therefore necessary to analyze multiple brain regions from diverse primate lineages to allow the identification of evolutionary patterns and innovations characteristic of each brain area. We paid particular attention to the non-cortical areas, which have rarely been studied at the genetic level, but which are known to have played key roles during the evolution of the primate brain. In this study, we utilized two classic indices that could be used to define a specific brain area in terms of its evolutionary rate and transcriptome age, with a view to identifying the evolutionary patterns and genetic changes characteristic of each brain area.

The phylostratigraphy approach has been used to trace the evolutionary origin of genes by similarity searches in genomes that represent the entire tree of life. The quantitative formula developed from this approach was the transcriptome age index which combined the phylostratum of a given gene with its expression data at a given developmental stage (Domazet-Loso et al. 2007; Domazet-Loso and Tautz, 2010). Employing the basic principle of this approach, we further utilized two classic formulae to calculate the evolutionary rate index (ERI) (Quint et al. 2012) and transcriptome age index (TAI) (Domazet-Loso et al. 2007;

Domazet-Loso and Tautz, 2010), thereby providing an effective means to study evolutionary changes in specific species.

It is well known that the evolutionary rates experienced by different primate brain areas and developmental stages are quite diverse. Indeed, previous research has shown that the cerebral cortex underwent rapid evolution in the primate lineage (Lui et al. 2011; Dehay et al. 2015). However, in this study, we unexpectedly found that the non-cortical areas evolved at an even faster rate than the cerebral cortex. The non-cortical areas constitute an essential part of the brain, responsible for the performance of complex functions and tasks such as emotions, motivation, learning, memory, and other advanced neural activities. The rapid evolution of the non-cortical areas may thus have been closely related to the evolutionary development of primate cognition and behavior. However, the evolution of the primate non-cortical areas has not been closely investigated. Those non-cortical areas that have evolved particularly rapidly, such as the hypophysis and the pineal gland, would clearly be worthy of further study.

Further, our results showed that *H. sapiens* and the Haplorrhini lineages exhibited markedly higher evolutionary rates than other primate lineages, indicating that the brains of *H. sapiens* and the Haplorrhini have undergone rapid evolution. Numerous studies have shown that the human brain evolved rapidly in terms of its relative volume and increased complexity through the expansion of cortical areas and an increase in density of cortical networks (King and Wilson, 1975; Pollard et al. 2006; Prabhakar et al. 2006; Bird et al. 2007; Boyd et al. 2015; Gittelman et al. 2015; Reilly et al. 2015; Dong et al. 2016; Won et al. 2019; Agoglia et al. 2021). What was unexpected was evidencing the rapid evolution of the Haplorrhini brain. However, previous research showed that the relative brain volume increased significantly in the Haplorrhini by comparison with the Strepsirrhini (Shao et al. 2023), which demonstrated that the cerebral cortex of the Haplorrhini brain has expanded rapidly whilst the brain volume of the Haplorrhini has significantly increased during the course of evolution. Our own research has additionally suggested that the Haplorrhini brain experienced rapid evolution, similar to *H. sapiens*.

We also observed that the evolutionary rates of the main brain regions during development display a mountain-like pattern reaching a peak during late infancy to early childhood. Although development continues into adulthood, the developmental stage from late infancy to early childhood is particularly important for the primate brain, since the foundations of adult sensory and perceptual systems which are essential to language, behavior, and emotion are formed at this stage. Our results indicate that the primate brain has experienced rapid evolution in the period from late infancy to early childhood; during this stage, the proliferation and migration of glial precursors, and the differentiation of astrocytes and oligodendrocytes, contribute to the functional maturation of the developing neural circuitry (Li and Barres, 2018), and hence may have promoted the evolution of the primate brain. Furthermore, the transcriptome ages of non-cortical areas were lower than those of the cerebral cortex, and each brain area was at its youngest during late infancy to early childhood, supporting the crucial roles of newly originated primate genes in brain development (Charrier et al. 2012; Dennis et al. 2012; Florio et al. 2015; Ju et al. 2016; Li et al. 2016; Liu et al. 2017; Heide et al. 2020).

In summary, our study reveals uneven evolutionary rates and transcriptome ages across different primate brain regions and developmental stages, indicating that the rewiring programs acting on the gene expression networks in the non-cortical areas and during infancy/early childhood have constituted crucial evolutionary steps toward acquiring our uniquely exceptional brain functions. This study deepens our understanding of brain evolution in primates, and particularly in humans.

Materials and Methods

Evolutionary Rate Index (ERI) Formula

To determine the evolutionary rate index (ERI) of different brain regions and developmental stages, we utilized the following formula (Quint et al. 2012):

$$\mathrm{ERI} = \frac{\sum_i^n \left(\frac{\mathrm{dN}}{\mathrm{dS}}\right)_i \times E_i}{\sum_i^n E_i}$$

where $(\mathrm{dN/dS})_i$ is a value that represents the ratio of nonsynonymous to synonymous mutations of a given gene i in a specific lineage, E_i is the expression value of gene i in a specific brain area, and n is the total number of genes analyzed. This formula was used to determine the evolutionary rate index of a particular brain area in a specific primate lineage. Where a particular tissue or developmental stage is described by a high ERI value, this is indicative of a high evolutionary rate for that tissue or stage. To ensure both the representativeness and accuracy of the results, we calculated the ERI index based on gene expression data from human and rhesus macaque, separately (Fig. 1A and C, supplementary tables S1 and S2, Supplementary Material online). A normalized gene expression matrix for human brain was obtained from the GTEx project (release V8) (GTEx Consortium 2020), which included 2,642 samples representing a total of 12 brain areas. The raw transcriptomes of rhesus macaque brain were obtained from the dataset published by our own laboratory (Li et al. 2019). The 590 transcriptomes

representing 45 brain areas were re-mapped to the reference genome (*Macaca mulatta*, Mmul_10, Ensembl v99) using STAR (Dobin et al. 2013) without providing junction annotation; those samples with >10 million uniquely mapped reads, and with the proportion of uniquely mapped reads being greater than 80%, were retained. Finally, the remaining 566 transcriptomes were used for downstream analyses (supplementary table S3, Supplementary Material online). We normalized the expression counts and calculated the TPM (transcript per million) for further analyses. The dN/dS values of 10,279 orthologous genes of *H. sapiens*, Hominini, Homininae, Hominidae, Hominoidea, Catarrhini, Simiiformes, and Haplorrhini were obtained from our laboratory's previously published paper (Shao et al. 2023); the orthologous genes were identified between human (*H. sapiens*, GRCh38), each of the other primate species and the outgroup species, the Chinese tree shrew, based on criteria including reciprocal best blastp hit (RBH), gene synteny and genome synteny (Shao et al. 2023). The evolutionary rate index yielded similar results whether based upon the human or the rhesus macaque brain transcriptome, indicating that our method was robust (Fig. 1A and C, supplementary tables S1 and S2, Supplementary Material online).

In addition, the ERI formula was also used to evaluate the evolutionary rates of different brain areas at different developmental stages. Normalized gene expression values of developing human brains were obtained from the previously published paper (Zhu et al. 2018); we selected 577 transcriptomes from six brain regions employing 8 developmental windows ranging from 12 pcw to 64 py.

Transcriptome Age Index (TAI) Formula

We evaluated the transcriptome age index (TAI) of different brain areas and developmental stages using the formula (Domazet-Loso and Tautz, 2003; Domazet-Loso et al. 2007):

$$\mathrm{TAI} = \frac{\sum_i^n A_i \times E_i}{\sum_i^n E_i}$$

where A_i is a value that represents the evolutionary age of a given gene i, i.e. the estimated time since the emergence of that gene according to phylogenetic analysis, E_i is the expression value of gene i within a specific brain area, and n is the total number of genes analyzed. When a brain area or developmental stage is described by a low TAI value, it indicates enrichment of evolutionarily young genes in that area or at that stage. We dated the origin of human protein-coding genes from the hg38 genome assembly based on the previously described pipelines (Zhang et al. 2011; Shao et al. 2019) from our other paper (Shao et al. 2023). Normalized gene expression values of adult human brains and developing human brains were derived from previously published papers (Zhu et al. 2018; GTEx Consortium 2020). To calculate more reliable ERI and TAI values, we did not set any expression cutoff for the expression data.

Supplementary Material

Supplementary material is available at *Genome Biology and Evolution* online.

Acknowledgments

We are grateful to the many individuals in our host institutions who have provided support to this project.

Funding

This work was supported by the Ministry of Science and Technology of the People Republic of China (SQ2023YFA 1800025), the CAS Light of West China Program (xbzg-zdsys-202213), and the Yunnan Provincial Department of Science and Technology (202305AH340006, 2019FI010, 2019FA008, and 2019FJ003).

Conflict of Interest

The authors are unaware of any competing interests.

Data Availability

All the data used in the manuscript were downloaded from previously published studies, as mentioned in the main text. Part of the analysis results were shown in the supplementary tables.

Literature Cited

Agoglia RM, Sun D, Birey F, Yoon SJ, Miura Y, Sabatini K, Pa?ca SP, Fraser HB. Primate cell fusion disentangles gene regulatory divergence in neurodevelopment. Nature. 2021:592(7854):421–427. https://doi.org/10.1038/s41586-021-03343-3.

Alatzoglou KS, Gregory LC, Dattani MT. Development of the pituitary gland. Compr Physiol. 2020:10(2):389–413. https://doi.org/10.1002/cphy.c150043.

Amiri A, Coppola G, Scuderi S, Wu F, Roychowdhury T, Liu F, Pochareddy S, Shin Y, Safi A, Song L, et al. Transcriptome and epigenome landscape of human cortical development modeled in organoids. Science. 2018:362(6420):eaat6720. https://doi.org/10.1126/science.aat6720.

Bakken TE, Miller JA, Ding SL, Sunkin SM, Smith KA, Ng L, Szafer A, Dalley RA, Royall JJ, Lemon T, et al. A comprehensive transcriptional map of primate brain development. Nature. 2016:535(7612):367–375. https://doi.org/10.1038/nature18637.

Barger N, Hanson KL, Teffer K, Schenker-Ahmed NM, Semendeferi K. Evidence for evolutionary specialization in human limbic structures. Front Hum Neurosci. 2014:8:277. https://doi.org/10.3389/fnhum.2014.00277.

Bernard A, Lubbers LS, Tanis KQ, Luo R, Podtelezhnikov AA, Finney EM, McWhorter MME, Serikawa K, Lemon T, Morgan R, et al.

Transcriptional architecture of the primate neocortex. Neuron. 2012:73(6):1083–1099. https://doi.org/10.1016/j.neuron.2012.03.002.
Bhaduri A, Sandoval-Espinosa C, Otero-Garcia M, Oh I, Yin R, Eze UC, Nowakowski TJ, Kriegstein AR. An atlas of cortical arealization identifies dynamic molecular signatures. Nature. 2021:598(7879):200–204. https://doi.org/10.1038/s41586-021-03910-8.
Bird CP, Stranger BE, Liu M, Thomas DJ, Ingle CE, Beazley C, Miller W, Hurles ME, Dermitzakis ET. Fast-evolving noncoding sequences in the human genome. Genome Biol. 2007:8(6):R118. https://doi.org/10.1186/gb-2007-8-6-r118.
Blaauw J, Meiners LC. The splenium of the corpus callosum: embryology, anatomy, function and imaging with pathophysiological hypothesis. Neuroradiology. 2020:62(5):563–585. https://doi.org/10.1007/s00234-019-02357-z.
Boyd JL, Skove SL, Rouanet JP, Pilaz LJ, Bepler T, Gordan R, Wray GA, Silver DL. Human–chimpanzee differences in a *FZD8* enhancer alter cell-cycle dynamics in the developing neocortex. Curr Biol. 2015:25(6):772–779. https://doi.org/10.1016/j.cub.2015.01.041.
Buckingham JC. The endocrine function of the hypothalamus. J Pharm Pharmacol. 1977:29(1):649–656. https://doi.org/10.1111/j.2042-7158.1977.tb11429.x.
Charrier C, Joshi K, Coutinho-Budd J, Kim JE, Lambert N, de Marchena J, Jin W-L, Vanderhaeghen P, Ghosh A, Sassa T, et al. Inhibition of *SRGAP2* function by its human-specific paralogs induces neoteny during spine maturation. Cell. 2012:149(4):923–935. https://doi.org/10.1016/j.cell.2012.03.034.
Chen S, Krinsky BH, Long M. New genes as drivers of phenotypic evolution. Nat Rev Genet. 2013:14(9):645–660. https://doi.org/10.1038/nrg3521.
Choi IG, Kim SH. Evolution of protein structural classes and protein sequence families. Proc Natl Acad Sci U S A. 2006:103(38):14056–-14061. https://doi.org/10.1073/pnas.0606239103.
DeCasien AR, Higham JP. Primate mosaic brain evolution reflects selection on sensory and cognitive specialization. Nat Ecol Evol. 2019:3(10):1483–1493. https://doi.org/10.1038/s41559-019-0969-0.
Dehay C, Kennedy H, Kosik KS. The outer subventricular zone and primate-specific cortical complexification. Neuron. 2015:85(4):683–694. https://doi.org/10.1016/j.neuron.2014.12.060.
Dennis MY, Nuttle X, Sudmant PH, Antonacci F, Graves TA, Nefedov M, Rosenfeld JA, Sajjadian S, Malig M, Kotkiewicz H, et al. Evolution of human-specific neural *SRGAP2* genes by incomplete segmental duplication. Cell. 2012:149(4):912–922. https://doi.org/10.1016/j.cell.2012.03.033.
Dobin A, Davis CA, Schlesinger F, Drenkow J, Zaleski C, Jha S, Batut P, Chaisson M, Gingeras TR. STAR: ultrafast universal RNA-seq aligner. Bioinformatics. 2013:29(1):15–21. https://doi.org/10.1093/bioinformatics/bts635.
Domazet-Loso T, Brajkovic J, Tautz D. A phylostratigraphy approach to uncover the genomic history of major adaptations in metazoan lineages. Trends Genet. 2007:23(11):533–539. https://doi.org/10.1016/j.tig.2007.08.014.
Domazet-Loso T, Tautz D. An evolutionary analysis of orphan genes in *Drosophila*. Genome Res. 2003:13(10):2213–2219. https://doi.org/10.1101/gr.1311003.
Domazet-Loso T, Tautz D. A phylogenetically based transcriptome age index mirrors ontogenetic divergence patterns. Nature. 2010:468(7325):815–818. https://doi.org/10.1038/nature09632.
Dong X, Wang X, Zhang F, Tian W. Genome-wide identification of regulatory sequences undergoing accelerated evolution in the human genome. Mol Biol Evol. 2016:33(10):2565–2575. https://doi.org/10.1093/molbev/msw128.
Dorus S, Vallender EJ, Evans PD, Anderson JR, Gilbert SL, Mahowald M, Wyckoff GJ, Malcom CM, Lahn BT. Accelerated evolution of nervous system genes in the origin of *Homo sapiens*. Cell. 2004:119(7):1027–1040. https://doi.org/10.1016/j.cell.2004.11.040.
Florio M, Albert M, Taverna E, Namba T, Brandl H, Lewitus E, Haffner C, Sykes A, Wong FK, Peters J, et al. Human-specific gene *ARHGAP11B* promotes basal progenitor amplification and neocortex expansion. Science. 2015:347(6229):1465–1470. https://doi.org/10.1126/science.aaa1975.
Force A, Lynch M, Pickett FB, Amores A, Yan YL, Postlethwait J. Preservation of duplicate genes by complementary, degenerative mutations. Genetics. 1999:151(4):1531–1545. https://doi.org/10.1093/genetics/151.4.1531.
Geirsdottir L, David E, Keren-Shaul H, Weiner A, Bohlen SC, Neuber J, Balic A, Giladi A, Sheban F, Dutertre C-A, et al. Cross-species single-cell analysis reveals divergence of the primate microglia program. Cell. 2020:181(3):746. https://doi.org/10.1016/j.cell.2020.04.002.
Gilad Y, Oshlack A, Smyth GK, Speed TP, White KP. Expression profiling in primates reveals a rapid evolution of human transcription factors. Nature. 2006:440(7081):242–245. https://doi.org/10.1038/nature04559.
Gilmore JH, Knickmeyer RC, Gao W. Imaging structural and functional brain development in early childhood. Nat Rev Neurosci. 2018:19(3):123–137. https://doi.org/10.1038/nrn.2018.1.
Gittelman RM, Hun E, Ay F, Madeoy J, Pennacchio L, Noble WS, Hawkins RD, Akey JM. Comprehensive identification and analysis of human accelerated regulatory DNA. Genome Res. 2015:25(9):1245–1255. https://doi.org/10.1101/gr.192591.115.
GTEx Consortium. The GTEx consortium atlas of genetic regulatory effects across human tissues. Science. 2020:369(6509):1318–1330. https://doi.org/10.1126/science.aaz1776.
Hawrylycz MJ, Lein ES, Guillozet-Bongaarts AL, Shen EH, Ng L, Miller JA, van de Lagemaat LN, Smith KA, Ebbert A, Riley ZL, et al. An anatomically comprehensive atlas of the adult human brain transcriptome. Nature. 2012:489(7416):391–399. https://doi.org/10.1038/nature11405.
He ZS, Han DD, Efimova O, Guijarro P, Yu QH, Oleksiak A, Jiang S, Anokhin K, Velichkovsky B, Grünewald S, et al. Comprehensive transcriptome analysis of neocortical layers in humans, chimpanzees and macaques. Nat Neurosci. 2017:20(6):886–895. https://doi.org/10.1038/nn.4548.
Heide M, Haffner C, Murayama A, Kurotaki Y, Shinohara H, Okano H, Sasaki E, Huttner WB. Human-specific *ARHGAP11B* increases size and folding of primate neocortex in the fetal marmoset. Science. 2020:369(6503):546–550. https://doi.org/10.1126/science.abb2401.
Ju XC, Hou QQ, Sheng AL, Wu KY, Zhou Y, Jin Y, Wen T, Yang Z, Wang X, Luo Z-G. The hominoid-specific gene *TBC1D3* promotes generation of basal neural progenitors and induces cortical folding in mice. Elife. 2016:5:e18197. https://doi.org/10.7554/eLife.18197.
Kanton S, Boyle MJ, He ZS, Santel M, Weigert A, Sanchis-Calleja F, Guijarro P, Sidow L, Fleck JS, Han D, et al. Organoid single-cell genomic atlas uncovers human-specific features of brain development. Nature. 2019:574(7778):418–422. https://doi.org/10.1038/s41586-019-1654-9.
King M-C, Wilson AC. Evolution at two levels in humans and chimpanzees. Science. 1975:188(4184):107–116. https://doi.org/10.1126/science.1090005.
Kronenberg ZN, Fiddes IT, Gordon D, Murali S, Cantsilieris S, Meyerson OS, Underwood JG, Nelson BJ, Chaisson MJP, Dougherty ML, et al. High-resolution comparative analysis of great ape genomes. Science. 2018:360(6393):eaar6343. https://doi.org/10.1126/science.aar6343.
Li ML, Wu SH, Zhang JJ, Tian HY, Shao Y, Wang ZB, Irwin DM, Li J-L, Hu X-T, Wu D-D. 547 transcriptomes from 44 brain areas reveal

features of the aging brain in non-human primates. Genome Biol. 2019:20(1):258. https://doi.org/10.1186/s13059-019-1866-1.
Li Q, Guo S, Jiang X, Bryk J, Naumann R, Enard W, Tomita M, Sugimoto M, Khaitovich P, Pääbo S. Mice carrying a human *GLUD2* gene recapitulate aspects of human transcriptome and metabolome development. Proc Natl Acad Sci U S A. 2016:113(19):5358–5363. https://doi.org/10.1073/pnas.1519261113.
Li QY, Barres BA. Microglia and macrophages in brain homeostasis and disease. Nat Rev Immunol. 2018:18(4):225–242. https://doi.org/10.1038/nri.2017.125.
Liu J, Liu W, Yang L, Wu Q, Zhang H, Fang A, Li L, Xu X, Sun L, Zhang J, et al. The primate-specific gene *TMEM14B* marks outer radial glia cells and promotes cortical expansion and folding. Cell Stem Cell. 2017:21(5):635–649.e8. https://doi.org/10.1016/j.stem.2017.08.013.
Long M, Betran E, Thornton K, Wang W. The origin of new genes: glimpses from the young and old. Nat Rev Genet. 2003:4(11):865–875. https://doi.org/10.1038/nrg1204.
Lovick TA, Li P. Integrated function of neurones in the rostral ventrolateral medulla. Prog Brain Res. 1989:81:223–232. https://doi.org/10.1016/S0079-6123(08)62012-9.
Lui JH, Hansen DV, Kriegstein AR. Development and evolution of the human neocortex. Cell. 2011:146(1):18–36. https://doi.org/10.1016/j.cell.2011.06.030.
Patel S, Rahmani B, Gandhi J, Seyam O, Joshi G, Reid I, Smith NL, Waltzer WC, Khan SA. Revisiting the pineal gland: a review of calcification, masses, precocious puberty, and melatonin functions. Int J Neurosci. 2020:130(5):464–475. https://doi.org/10.1080/00207454.2019.1692838.
Paul LK, Brown WS, Adolphs R, Tyszka JM, Richards LJ, Mukherjee P, Sherr EH. Agenesis of the corpus callosum: genetic, developmental and functional aspects of connectivity. Nat Rev Neurosci. 2007:8(4):287–299. https://doi.org/10.1038/nrn2107.
Pelletier D, Neuman MJ. Advancing the nutrition and early childhood development agenda: indicators and guidance. Ann N Y Acad Sci. 2014:1308(1):232–244. https://doi.org/10.1111/nyas.12288.
Phansuwan-Pujito P, Moller M, Govitrapong P. Cholinergic innervation and function in the mammalian pineal gland. Microsc Res Tech. 1999:46(4-5):281–295. https://doi.org/10.1002/(SICI)1097-0029(19990815/01)46:4/5<281::AID-JEMT5>3.0.CO;2-N.
Pickles JO. Auditory pathways: anatomy and physiology. Handb Clin Neurol. 2015:129:3–25. https://doi.org/10.1016/B978-0-444-62630-1.00001-9.
Pollard KS, Salama SR, King B, Kern AD, Dreszer T, Katzman S, Siepel A, Pedersen JS, Bejerano G, Baertsch R, et al. Forces shaping the fastest evolving regions in the human genome. PLoS Genet. 2006:2(10):1599–1611. https://doi.org/10.1371/journal.pgen.0020168.
Prabhakar S, Noonan JP, Pääbo S, Rubin EM. Accelerated evolution of conserved noncoding sequences in humans. Science. 2006:314(5800):786. https://doi.org/10.1126/science.1130738.
Quint M, Drost HG, Gabel A, Ullrich KK, Bonn M, Grosse I. A transcriptomic hourglass in plant embryogenesis. Nature. 2012:490(7418):98–101. https://doi.org/10.1038/nature11394.
Reilly SK, Yin J, Ayoub AE, Emera D, Leng J, Cotney J, Sarro R, Rakic P, Noonan JP. Evolutionary changes in promoter and enhancer activity during human corticogenesis. Science. 2015:347(6226):1155–1159. https://doi.org/10.1126/science.1260943.
Sapede D, Cau E. The pineal gland from development to function. Curr Top Dev Biol. 2013:106:171–215. https://doi.org/10.1016/B978-0-12-416021-7.00005-5.
Shao Y, Chen CY, Shen H, He BZ, Yu DQ, Jiang S, Zhao S, Gao Z, Zhu Z, Chen X, et al. GenTree, an integrated resource for analyzing the evolution and function of primate-specific coding genes. Genome Res. 2019:29(4):682–696. https://doi.org/10.1101/gr.238733.118.
Shao Y, Zhou L, Li F, Zhao L, Zhang B-L, Shao F, Chen J-W, Chen C-Y, Bi X, Zhuang X-L, et al. Phylogenomic analyses provide insights into primate evolution. Science. 2023:380(6648):913–924. https://doi.org/10.1126/science.abn6919.
Sousa AMM, Meyer KA, Santpere G, Gulden FO, Sestan N. Evolution of the human nervous system function, structure, and development. Cell. 2017a:170(2):226–247. https://doi.org/10.1016/j.cell.2017.06.036.
Sousa AMM, Zhu Y, Raghanti MA, Kitchen RR, Onorati M, Tebbenkamp ATN, Stutz B, Meyer KA, Li M, Kawasawa YI, et al. Molecular and cellular reorganization of neural circuits in the human lineage. Science. 2017b:358(6366):1027–1032. https://doi.org/10.1126/science.aan3456.
Trachtman JN. Vision and the hypothalamus. Optometry. 2010:81(2):100–115. https://doi.org/10.1016/j.optm.2009.07.016.
Tuller T, Kupiec M, Ruppin E. Evolutionary rate and gene expression across different brain regions. Genome Biol. 2008:9(9):R142. https://doi.org/10.1186/gb-2008-9-9-r142.
Vijayakumar N, Op de Macks Z, Shirtcliff EA, Pfeifer JH. Puberty and the human brain: insights into adolescent development. Neurosci Biobehav Rev. 2018:92:417–436. https://doi.org/10.1016/j.neubiorev.2018.06.004.
Won H, Huang J, Opland CK, Hartl CL, Geschwind DH. Human evolved regulatory elements modulate genes involved in cortical expansion and neurodevelopmental disease susceptibility. Nat Commun. 2019:10(1):2396. https://doi.org/10.1038/s41467-019-10248-3.
Wurtz RH, Albano JE. Visual-motor function of the primate superior colliculus. Annu Rev Neurosci. 1980:3(1):189–226. https://doi.org/10.1146/annurev.ne.03.030180.001201.
Zhang YE, Landback P, Vibranovski MD, Long MY. Accelerated recruitment of new brain development genes into the human genome. PLoS Biol. 2011:9(10):e1001179. https://doi.org/10.1371/journal.pbio.1001179.
Zhu Y, Sousa AMM, Gao TLY, Skarica M, Li MF, Santpere G, Esteller-Cucala P, Juan D, Ferrández-Peral L, Gulden FO, et al. Spatiotemporal transcriptomic divergence across human and macaque brain development. Science. 2018:362(6420):eaat8077. https://doi.org/10.1126/science.aat8077.

Associate editor: Soojin Yi

Supplementary Tables Legends

Table S1	Evolutionary rate index of specific brain areas in a specific primate lineage based on macaque brain gene expression data
Table S2	Evolutionary rate index of specific brain areas in a specific primate lineage based on human brain gene expression data
Table S3	Information of 590 rhesus macaque brain samples (deleted samples were filled with darkgreen)
Table S4	Evolutionary rate index of specific brain areas in a specific primate lineage at specific developmental stages of human
Table S5	Transcriptome age index of specific brain areas of human
Table S6	Transcriptome age index of specific brain areas of human at specific developmental stages

Macaque brain areas / Lineages	CN	PTM	GP	AMY	HIP	CGS	TH	HTH	SC	IC
Homo sapiens	69.14568	68.63184	69.92294	68.5493	68.29807	68.37106	69.33732	70.07771	70.09953	70.39781
Hominini	53.27185	52.87783	54.38033	52.12319	52.23077	52.15237	52.41769	53.90708	53.62418	53.74486
Homininae	44.28469	44.08645	45.20703	43.69496	43.49979	43.57643	44.17829	44.50566	44.49371	44.81539
Hominidae	60.81951	60.45804	62.51348	59.97668	60.12119	59.64719	60.40957	62.05599	61.75773	62.10618
Hominoidea	41.99935	41.78198	42.68098	40.94063	41.02509	40.93264	41.20164	42.03735	41.81024	42.08505
Catarrhini	30.37159	30.02345	29.96252	29.53761	29.44434	29.19468	29.4771	29.91255	29.66755	29.9373
Simiiformes	5.280549	5.221705	5.180466	5.145325	5.070123	5.075935	5.247153	5.409478	5.266244	5.334456
Haplorrhini	62.50276	62.29285	62.81489	61.86552	61.46469	61.35921	61.96778	63.11252	62.65036	62.75677

Macaque brain areas / Lineages	pons	CV	HYP	ACB	CC	VTA	OB	MED	PG	SU	IPS	LF	PEC	AMG	AG
Homo sapiens	69.88643	68.45824	72.28822	68.8907	70.47686	69.76228	69.09264	71.07515	72.49691	68.60965	68.61918	68.43114	68.7156	68.77763	68.63877
Hominini	53.55088	51.74223	56.10696	53.33648	54.75951	53.80393	53.64144	54.44847	55.05855	52.25915	52.33319	52.2999	52.43566	52.371	52.06604
Homininae	45.30619	43.79064	46.49361	43.87501	45.30719	44.40946	44.09801	45.45728	45.90606	43.71739	43.75621	43.60459	43.78502	43.92979	43.6427
Hominidae	62.79128	59.3278	64.06716	60.47276	63.25897	61.77887	61.02098	62.90682	64.33224	59.78379	59.98484	59.74965	59.86317	59.96793	59.62675
Hominoidea	42.20597	40.64651	42.8533	41.57341	42.9757	41.7827	41.63976	42.79886	43.26588	40.94782	40.94265	40.7773	41.10437	41.05548	40.8899
Catarrhini	29.99384	28.67952	30.58501	30.119	29.61017	29.89069	29.32155	30.19311	30.29625	29.0064	29.05931	28.95237	29.13118	29.18526	28.95608
Simiiformes	5.187395	5.138895	5.225152	5.382146	5.201655	5.279082	5.494562	5.525427	5.167698	4.983645	4.996821	5.028797	5.026316	5.044588	5.015108
Haplorrhini	62.46655	60.83442	65.34988	62.80676	62.56898	62.55751	62.42515	63.23931	65.43492	61.2915	61.39343	61.561	61.47556	61.64076	61.38182

Macaque brain areas / Lineages	LSTG	TPG	DLPFC	VLPFC	ASPD	V1C	V2C	V4C	SFG	CBC
Homo sapiens	68.54126	68.32217	68.79276	68.75699	68.84069	68.6888	68.63091	68.66345	68.75986	68.58423
Hominini	52.33571	51.88875	52.47013	52.44853	52.3826	52.1414	52.13892	52.11694	52.34893	51.86023
Homininae	43.61143	43.4495	43.63725	43.90205	43.77228	43.73227	43.79071	43.69102	43.70578	43.97474
Hominidae	59.88443	59.55785	59.91772	60.05635	59.98615	59.76947	59.69354	59.73189	59.89027	59.5154
Hominoidea	40.95061	40.82847	41.03292	41.15976	41.06084	40.74582	40.78431	40.7675	41.04983	40.94007
Catarrhini	29.26362	28.96592	29.09026	29.20371	29.17163	28.9259	28.91756	28.96614	29.17514	28.73686
Simiiformes	5.028242	4.996868	5.099234	5.11833	5.098092	4.976018	4.950157	4.998858	5.090802	5.083926
Haplorrhini	61.75918	61.50115	61.56193	61.6669	61.74197	61.60325	61.62454	61.74232	61.45972	60.83085

Macaque brain areas / Lineages	VMPFC	AIC	PIC	OFC	PSPD	SAR	PS	ASD	ARSP	SPCD
Homo sapiens	68.43237	68.51928	68.53948	68.61301	68.75749	68.50613	68.48933	68.92658	68.82669	68.74343
Hominini	52.36295	52.29947	52.17591	52.21244	52.40715	52.24397	52.07413	52.33735	52.37544	52.37345
Homininae	43.52978	43.76804	43.63426	43.69615	43.76276	43.64412	43.58506	43.97913	44.11364	43.95253
Hominidae	59.82734	59.95358	59.73049	59.85923	60.02065	59.92825	59.70849	60.12929	60.20786	60.21004
Hominoidea	41.01605	40.99113	40.91562	41.03119	41.01084	41.05203	40.8991	41.14967	41.22902	41.12924
Catarrhini	29.23554	29.44996	29.14612	29.2673	29.25997	29.08597	28.98396	29.3193	29.39479	29.24455
Simiiformes	5.14428	5.141422	5.028439	5.080527	5.095617	5.053694	5.014503	5.063766	5.016881	5.058227
Haplorrhini	61.4916	61.83192	61.67567	61.40596	61.53496	61.40165	61.35162	61.43855	61.44376	61.57697

CN	Caudate nucleus
PTM	Putamen
GP	Global pallidum
AMY	Amygdala
HIP	Hippocampus
CGS	Cingulate sulcus
TH	Thalamus
HTH	Hypothalamus
SC	Superior colliculus
IC	Inferior colliculus
pons	Pons
CV	Cerebellar vermis
HYP	Hypophysis
ACB	Accumbens nucleus
CC	Corpus callosum
VTA	Ventral tegmental area
OB	Olfactory bulb
MED	Medulla
PG	Pineal gland
SU	Superior postcentral dimple
IPS	Intraparietal sulcus
LF	Lateral fissure
PEC	Parietal area
AMG	Anterior marginal gyrus
AG	Angular gyrus
LSTG	Lateral superior temporal gyrus
TPG	Temporal polar gyrus
DLPFC	Dorsolateral prefrontal cortex
VLPFC	Ventral lateral prefrontal cortex
ASPD	Anterior supraprincipal dimple
V1C	Primary visual cortex
V2C	Visual cortex V2
V4C	Visual cortex V4
SFG	Superior frontal gyrus
CBC	Cerebellar cortex
VMPFC	Ventromedial prefrontal cortex
AIC	Anterior insula cortex
PIC	Posterior insula cortex
OFC	Orbitofrontal cortex
PSPD	Posterior supraprincipal dimple
SAR	Superior arcuate sulcus
PS	Principal sulcus
ASD	Anterior subcentral dimple
ARSP	Arcuate sulcus spur
SPCD	Superior precentral dimple

Lineages \ Human brain areas	Cortex	FC	ACC	Cerebellum	AMY	HIP	PTM	ACB	CN	HTH	SN	SPC
Homo sapiens	69.552819	70.000736	69.968929	69.784642	70.665246	70.534255	71.0429	70.96473	71.141328	71.877297	71.952092	73.29902
Hominini	51.078697	50.798674	51.023873	51.581466	52.101248	51.990953	52.091427	52.400574	52.476961	52.753235	53.282179	54.08526
Homininae	44.641704	45.034393	45.207486	45.156312	46.164265	46.096589	46.20612	46.043329	46.32273	46.829576	47.616533	48.590837
Hominidae	59.818615	60.036121	60.193313	59.150555	61.305648	61.337066	61.314013	61.194815	61.811825	62.211334	63.078725	63.91569
Hominoidea	41.481914	41.944514	42.082633	41.99894	42.906983	42.856417	43.084631	43.114373	43.248481	43.430277	44.186404	45.157184
Catarrhini	30.17989	30.691791	30.982657	29.719016	31.423355	31.246736	31.665804	31.682781	31.672966	31.671311	32.094861	31.962799
Simiiformes	5.1905198	5.2240472	5.4305586	5.2991603	5.5735883	5.4107133	5.3957832	5.6230744	5.4379285	5.6529517	5.5009746	5.4751217
Haplorrhini	63.076192	63.280209	63.164799	62.93168	63.480462	63.298957	63.716982	64.14972	64.040321	65.386322	65.081778	65.899952

FC	Frontal cortex
ACC	Anterior cingulate cortex
AMY	Amygdala
HIP	Hippocampus
PTM	Putamen
ACB	Accumbens nucleus
CN	Caudate nucleus
HTH	Hypothalamus
SN	Substantia nigra
SPC	Spinal cord

Sample ID	Individual	Age	Sex	RIN	Tissues(full name)	Tissues(short name)	Uniquely mapped reads number	Uniquely mapped reads %
396-10L	ypa396	6	Female	7.4	Superior postcentral dimple	SU	12391205	84.40%
396-10R	ypa396	6	Female	8	Superior postcentral dimple	SU	12129450	83.30%
396-11L	ypa396	6	Female	7.9	Intraparietal sulcus	IPS	14782079	75.10%
396-11R	ypa396	6	Female	7.7	Intraparietal sulcus	IPS	23588184	86.90%
396-12L	ypa396	6	Female	8.1	Lateral fissure	LF	18948830	87.30%
396-12R	ypa396	6	Female	7.5	Lateral fissure	LF	13972797	88.40%
396-13L	ypa396	6	Female	6.4	Parietal area	PEC	11577452	82.00%
396-13R	ypa396	6	Female	7.7	Parietal area	PEC	14750659	87.40%
396-14L	ypa396	6	Female	8.1	Anterior marginal gyrus	AMG	12893021	86.00%
396-14R	ypa396	6	Female	8.4	Anterior marginal gyrus	AMG	17776055	86.40%
396-15L	ypa396	6	Female	8.3	Angular gyrus	AG	11823930	83.50%
396-15R	ypa396	6	Female	8.4	Angular gyrus	AG	16618734	87.30%
396-16L	ypa396	6	Female	7.6	Lateral superior temporal gyrus	LSTG	12862735	82.50%
396-16R	ypa396	6	Female	7.5	Lateral superior temporal gyrus	LSTG	12771384	84.80%
396-17L	ypa396	6	Female	7.7	Lateral superior temporal gyrus	LSTG	18261457	81.70%
396-17R	ypa396	6	Female	7.9	Lateral superior temporal gyrus	LSTG	12759958	86.20%
396-18L	ypa396	6	Female	8.3	Temporal polar gyrus	TPG	14831820	87.80%
396-18R	ypa396	6	Female	6.6	Temporal polar gyrus	TPG	13188047	84.10%
396-19L	ypa396	6	Female	7.5	Temporal polar gyrus	TPG	13552578	87.90%
396-19R	ypa396	6	Female	8.2	Temporal polar gyrus	TPG	17737399	86.30%
396-1L	ypa396	6	Female	7.8	Dorsolateral prefrontal cortex	DLPFC	13788243	86.80%
396-1R	ypa396	6	Female	7.9	Dorsolateral prefrontal cortex	DLPFC	13818222	86.40%
396-20L	ypa396	6	Female	5.6	Primary visual cortex	V1C	11461290	74.50%
396-20R	ypa396	6	Female	8.2	Primary visual cortex	V1C	16181793	87.70%
396-21L	ypa396	6	Female	7.1	Visual cortex V2	V2C	15934660	88.10%
396-21R	ypa396	6	Female	6.1	Visual cortex V2	V2C	13450993	86.60%
396-22L	ypa396	6	Female	7.3	Visual cortex V4	V4C	13156340	87.80%
396-22R	ypa396	6	Female	7.1	Visual cortex V4	V4C	14740308	86.60%
396-23L	ypa396	6	Female	7.7	Superior frontal gyrus	SFG	14568741	85.70%
396-23R	ypa396	6	Female	7.4	Superior frontal gyrus	SFG	15609676	85.30%
396-24L	ypa396	6	Female	8	Caudate nucleus	CN	16296267	86.80%
396-24R	ypa396	6	Female	8.4	Caudate nucleus	CN	13641560	84.50%
396-25L	ypa396	6	Female	7	Putamen	PTM	12686124	84.60%
396-25R	ypa396	6	Female	7.9	Putamen	PTM	15126621	83.00%
396-26L	ypa396	6	Female	7.3	Global pallidum	GP	15850941	85.00%
396-26R	ypa396	6	Female	7	Global pallidum	GP	13937682	85.10%
396-27L	ypa396	6	Female	8.2	Amygdala	AMY	13862334	88.80%
396-27R	ypa396	6	Female	6.9	Amygdala	AMY	15363029	84.80%
396-28L	ypa396	6	Female	7.7	Hippocampus	HIP	15998376	89.50%
396-28R	ypa396	6	Female	7.6	Hippocampus	HIP	14961847	87.60%
396-2L	ypa396	6	Female	7.3	Ventral lateral prefrontal cortex	VLPFC	20486344	86.20%
396-2R	ypa396	6	Female	7.4	Ventral lateral prefrontal cortex	VLPFC	13074602	84.40%
396-31L	ypa396	6	Female	6.4	Cingulate sulcus	CGS	10681458	73.80%
396-31R	ypa396	6	Female	7.9	Cingulate sulcus	CGS	18502545	86.60%
396-32	ypa396	6	Female	7.7	Thalamus	TH	12632837	86.10%
396-33	ypa396	6	Female	7.8	Hypothalamus	HTH	14153836	84.20%
396-34L	ypa396	6	Female	7.1	Superior colliculus	SC	18727559	87.50%
396-34R	ypa396	6	Female	8	Superior colliculus	SC	14365776	85.30%
396-35L	ypa396	6	Female	7.8	Inferior colliculus	IC	15071058	85.80%
396-35R	ypa396	6	Female	7.3	Inferior colliculus	IC	14586988	87.00%
396-37	ypa396	6	Female	6.9	pons	pons	16342201	86.40%
396-38L	ypa396	6	Female	NA	Cerebellar cortex	CBC	13719636	88.30%
396-38R	ypa396	6	Female	NA	Cerebellar cortex	CBC	12689373	86.90%
396-39	ypa396	6	Female	7.3	Cerebellar vermis	CV	14697653	84.60%
396-3L	ypa396	6	Female	8.1	Anterior supraprincipal dimple	ASPD	13816893	88.50%
396-3R	ypa396	6	Female	7.6	Anterior supraprincipal dimple	ASPD	13262998	86.80%
396-41	ypa396	6	Female	8.3	Hypophysis	HYP	14959345	91.80%
396-42L	ypa396	6	Female	7.3	Ventromedial prefrontal cortex	VMPFC	27340593	84.40%
396-42R	ypa396	6	Female	7.1	Ventromedial prefrontal cortex	VMPFC	14914683	88.30%
396-43L	ypa396	6	Female	7.7	Anterior insula cortex	AIC	16357156	85.40%
396-43R	ypa396	6	Female	8	Anterior insula cortex	AIC	17805528	88.00%
396-44L	ypa396	6	Female	7.5	Posterior insula cortex	PIC	20195675	87.90%
396-44R	ypa396	6	Female	7.9	Posterior insula cortex	PIC	17820582	87.30%
396-45L	ypa396	6	Female	7.6	Orbitofrontal cortex	OFC	14158771	89.30%
396-45R	ypa396	6	Female	7.9	Orbitofrontal cortex	OFC	15208903	88.60%
396-46R	ypa396	6	Female	7.3	Accumbens nucleus	ACB	14969213	86.90%
396-47L	ypa396	6	Female	8.2	Corpus callosum	CC	16075580	89.10%
396-47R	ypa396	6	Female	8.8	Corpus callosum	CC	16197936	89.50%
396-48-2	ypa396	6	Female	7.2	Ventral tegmental area	VTA	17047482	88.00%
396-49L	ypa396	6	Female	8.2	Olfactory bulb	OB	12110507	88.10%
396-49R	ypa396	6	Female	8.1	Olfactory bulb	OB	13892433	89.10%
396-4L	ypa396	6	Female	6.7	Posterior supraprincipal dimple	PSPD	14220154	85.00%
396-4R	ypa396	6	Female	7.2	Posterior supraprincipal dimple	PSPD	15107132	86.00%
396-53	ypa396	6	Female	7.8	Medulla	MED	14342130	89.70%
396-5L-2	ypa396	6	Female	7.3	Superior arcuate sulcus	SAR	35107016	87.30%
396-5R	ypa396	6	Female	7.1	Superior arcuate sulcus	SAR	14720677	86.20%
396-6L	ypa396	6	Female	7.6	Principal sulcus	PS	13187505	86.10%
396-6R	ypa396	6	Female	7.6	Principal sulcus	PS	13551041	83.00%
396-7L	ypa396	6	Female	7.5	Anterior subcentral dimple	ASD	14382142	85.80%
396-7R	ypa396	6	Female	7.1	Anterior subcentral dimple	ASD	18221225	86.80%
396-8L	ypa396	6	Female	7	Arcuate sulcus spur	ARSP	14919714	84.90%
396-8R	ypa396	6	Female	7.8	Arcuate sulcus spur	ARSP	18514795	88.70%
396-9L	ypa396	6	Female	7.5	Superior precentral dimple	SPCD	14741411	82.30%
396-9R	ypa396	6	Female	7.8	Superior precentral dimple	SPCD	13012951	85.20%
397-10	ypa397	6	Male	6.9	Superior postcentral dimple	SU	14363673	87.30%
397-10L	ypa397	6	Male	6.3	Superior postcentral dimple	SU	24041097	87.20%
397-11L	ypa397	6	Male	6.3	Intraparietal sulcus	IPS	14236597	85.71%
397-11R	ypa397	6	Male	7.4	Intraparietal sulcus	IPS	15817846	88.03%
397-12L	ypa397	6	Male	6.1	Lateral fissure	LF	11746825	85.40%
397-12R	ypa397	6	Male	6.7	Lateral fissure	LF	13624576	89.75%
397-13L-2	ypa397	6	Male	7.1	Parietal area	PEC	12366346	73.46%
397-13R	ypa397	6	Male	7	Parietal area	PEC	19355012	90.23%
397-14L	ypa397	6	Male	6.8	Anterior marginal gyrus	AMG	15738829	87.76%
397-14R	ypa397	6	Male	6.5	Anterior marginal gyrus	AMG	14895175	91.31%
397-15L	ypa397	6	Male	6.6	Angular gyrus	AG	16728238	88.22%
397-15R	ypa397	6	Male	7.4	Angular gyrus	AG	13690703	91.69%
397-16L	ypa397	6	Male	7.4	Lateral superior temporal gyrus	LSTG	13111007	87.01%
397-16R	ypa397	6	Male	6.8	Lateral superior temporal gyrus	LSTG	22677244	90.32%
397-17L	ypa397	6	Male	7.2	Lateral superior temporal gyrus	LSTG	13768775	86.60%
397-17R	ypa397	6	Male	6.2	Lateral superior temporal gyrus	LSTG	13099886	84.57%
397-18L	ypa397	6	Male	6.9	Temporal polar gyrus	TPG	15561375	87.95%
397-18R	ypa397	6	Male	7.2	Temporal polar gyrus	TPG	12294309	86.03%
397-19L	ypa397	6	Male	7.1	Temporal polar gyrus	TPG	12852776	87.55%

397-19R	ypa397	6	Male	7.1	Temporal polar gyrus	TPG	14403302	87.62%
397-1L	ypa397	6	Male	7.3	Dorsolateral prefrontal cortex	DLPFC	12360255	86.89%
397-1R	ypa397	6	Male	7.8	Dorsolateral prefrontal cortex	DLPFC	13432753	88.25%
397-20L	ypa397	6	Male	7.3	Primary visual cortex	V1C	12279136	85.17%
397-20R	ypa397	6	Male	7.5	Primary visual cortex	V1C	13558877	85.92%
397-21L	ypa397	6	Male	7.2	Visual cortex V2	V2C	15419209	87.19%
397-21R	ypa397	6	Male	7.4	Visual cortex V2	V2C	13576079	87.80%
397-22L	ypa397	6	Male	6.8	Visual cortex V4	V4C	15557574	87.94%
397-22R	ypa397	6	Male	7.6	Visual cortex V4	V4C	15349041	87.61%
397-23L	ypa397	6	Male	6.8	Superior frontal gyrus	SFG	15464838	88.00%
397-23R	ypa397	6	Male	7.1	Superior frontal gyrus	SFG	16194713	86.27%
397-24L	ypa397	6	Male	8.2	Caudate nucleus	CN	15293940	86.07%
397-24R	ypa397	6	Male	8.6	Caudate nucleus	CN	11592388	85.60%
397-25L	ypa397	6	Male	8.1	Putamen	PTM	13642228	85.94%
397-25R	ypa397	6	Male	7.2	Putamen	PTM	14213962	84.20%
397-26L	ypa397	6	Male	8.3	Global pallidum	GP	13099618	88.33%
397-26R-2	ypa397	6	Male	7.2	Global pallidum	GP	11566446	72.27%
397-27L	ypa397	6	Male	7.4	Amygdala	AMY	12733415	88.22%
397-27R	ypa397	6	Male	7.3	Amygdala	AMY	12595901	87.22%
397-28L	ypa397	6	Male	6.4	Hippocampus	HIP	11272652	76.27%
397-28R	ypa397	6	Male	7.2	Hippocampus	HIP	16632022	87.01%
397-2L	ypa397	6	Male	6.7	Ventral lateral prefrontal cortex	VLPFC	12684392	85.39%
397-2R	ypa397	6	Male	7.3	Ventral lateral prefrontal cortex	VLPFC	13183569	87.81%
397-31L	ypa397	6	Male	8	Cingulate sulcus	CGS	15514749	86.95%
397-31R	ypa397	6	Male	7.1	Cingulate sulcus	CGS	12346542	87.39%
397-32	ypa397	6	Male	6.6	Thalamus	TH	15600394	86.75%
397-33	ypa397	6	Male	6.7	Hypothalamus	HTH	12827472	85.63%
397-34L	ypa397	6	Male	7.3	Superior colliculus	SC	13777433	84.95%
397-34R	ypa397	6	Male	7.7	Superior colliculus	SC	16571188	87.70%
397-35L	ypa397	6	Male	7.2	Inferior colliculus	IC	14932344	85.94%
397-35R	ypa397	6	Male	7.6	Inferior colliculus	IC	21316272	87.47%
397-37	ypa397	6	Male	6.7	pons	pons	15179956	87.82%
397-38L	ypa397	6	Male	7.1	Cerebellar cortex	CBC	15603093	87.19%
397-38R	ypa397	6	Male	8.2	Cerebellar cortex	CBC	16704833	88.66%
397-39	ypa397	6	Male	8.3	Cerebellar vermis	CV	13079793	89.54%
397-3L	ypa397	6	Male	6.6	Anterior supraprincipal dimple	ASPD	14044848	87.14%
397-3R	ypa397	6	Male	7.2	Anterior supraprincipal dimple	ASPD	15593762	87.80%
397-40	ypa397	6	Male	9	Pineal gland	PG	16882799	89.13%
397-41	ypa397	6	Male	9	Hypophysis	HYP	12836464	88.53%
397-42L	ypa397	6	Male	7.1	Ventromedial prefrontal cortex	VMPFC	15191847	85.10%
397-42R	ypa397	6	Male	7.4	Ventromedial prefrontal cortex	VMPFC	15190253	87.50%
397-43L	ypa397	6	Male	7.1	Anterior insula cortex	AIC	12070321	83.74%
397-43R	ypa397	6	Male	7.8	Anterior insula cortex	AIC	12848121	88.54%
397-44L-2	ypa397	6	Male	6.8	Posterior insula cortex	PIC	12212586	74.38%
397-44R	ypa397	6	Male	7.1	Posterior insula cortex	PIC	12392542	86.67%
397-45L	ypa397	6	Male	6.7	Orbitofrontal cortex	OFC	17186131	85.35%
397-45R	ypa397	6	Male	6.7	Orbitofrontal cortex	OFC	13760179	87.89%
397-46L	ypa397	6	Male	7.1	Accumbens nucleus	ACB	13058946	85.15%
397-46R	ypa397	6	Male	7.4	Accumbens nucleus	ACB	12044546	83.84%
397-47L	ypa397	6	Male	8.5	Corpus callosum	CC	15297686	87.83%
397-47R	ypa397	6	Male	8.4	Corpus callosum	CC	14518804	88.76%
397-48	ypa397	6	Male	7.7	Ventral tegmental area	VTA	15505356	87.21%
397-49L	ypa397	6	Male	6.6	Olfactory bulb	OB	15494169	86.35%
397-49R	ypa397	6	Male	6.8	Olfactory bulb	OB	12830741	88.47%
397-4L	ypa397	6	Male	7.2	Posterior supraprincipal dimple	PSPD	13774901	87.73%
397-4R	ypa397	6	Male	7.5	Posterior supraprincipal dimple	PSPD	16617883	87.74%
397-5L	ypa397	6	Male	6.9	Superior arcuate sulcus	SAR	13469389	85.20%
397-5R	ypa397	6	Male	7.4	Superior arcuate sulcus	SAR	15803526	89.24%
397-6L	ypa397	6	Male	7	Principal sulcus	PS	14583982	86.59%
397-6R	ypa397	6	Male	7.4	Principal sulcus	PS	19305393	85.84%
397-7L	ypa397	6	Male	6.8	Anterior subcentral dimple	ASD	17042351	86.59%
397-7R	ypa397	6	Male	6	Anterior subcentral dimple	ASD	13551492	88.11%
397-8L	ypa397	6	Male	6.8	Arcuate sulcus spur	ARSP	31132330	86.76%
397-8R	ypa397	6	Male	6.8	Arcuate sulcus spur	ARSP	13734839	89.99%
397-9L	ypa397	6	Male	6.5	Superior precentral dimple	SPCD	17610451	86.77%
397-9R	ypa397	6	Male	7	Superior precentral dimple	SPCD	13855324	89.33%
398-10L	ypa398	6	Female	7.5	Superior postcentral dimple	SU	15286203	86.34%
398-10R	ypa398	6	Female	7.2	Superior postcentral dimple	SU	13460453	87.47%
398-11L	ypa398	6	Female	7.5	Intraparietal sulcus	IPS	14811005	85.70%
398-11R	ypa398	6	Female	7	Intraparietal sulcus	IPS	13475503	88.03%
398-12L	ypa398	6	Female	8.1	Lateral fissure	LF	14936280	85.71%
398-12R	ypa398	6	Female	7.1	Lateral fissure	LF	17348821	89.00%
398-13L	ypa398	6	Female	7.7	Parietal area	PEC	14665585	87.95%
398-13R	ypa398	6	Female	6.8	Parietal area	PEC	13688363	87.13%
398-14L	ypa398	6	Female	7.4	Anterior marginal gyrus	AMG	14868660	86.56%
398-14R	ypa398	6	Female	7.4	Anterior marginal gyrus	AMG	13131731	87.85%
398-15L	ypa398	6	Female	7.3	Angular gyrus	AG	13508267	87.87%
398-15R	ypa398	6	Female	6.9	Angular gyrus	AG	13285155	87.53%
398-16L	ypa398	6	Female	7.6	Lateral superior temporal gyrus	LSTG	16891281	88.04%
398-16R	ypa398	6	Female	7.8	Lateral superior temporal gyrus	LSTG	13915255	83.82%
398-17L	ypa398	6	Female	7.4	Lateral superior temporal gyrus	LSTG	15577949	88.08%
398-17R	ypa398	6	Female	7.9	Lateral superior temporal gyrus	LSTG	14930488	86.16%
398-18L	ypa398	6	Female	7.1	Temporal polar gyrus	TPG	14458754	86.79%
398-18R	ypa398	6	Female	8.2	Temporal polar gyrus	TPG	14440560	85.58%
398-19L-2	ypa398	6	Female	7.6	Temporal polar gyrus	TPG	18677510	88.83%
398-19R	ypa398	6	Female	7.4	Temporal polar gyrus	TPG	13588686	85.54%
398-1L	ypa398	6	Female	6.8	Dorsolateral prefrontal cortex	DLPFC	13979553	85.89%
398-1R	ypa398	6	Female	7.6	Dorsolateral prefrontal cortex	DLPFC	13674370	85.16%
398-20L	ypa398	6	Female	6.3	Primary visual cortex	V1C	18082221	89.20%
398-20R	ypa398	6	Female	8.4	Primary visual cortex	V1C	15284532	86.76%
398-21L	ypa398	6	Female	7	Visual cortex V2	V2C	15770442	88.46%
398-21R	ypa398	6	Female	7.7	Visual cortex V2	V2C	14212964	84.98%
398-22L	ypa398	6	Female	6.6	Visual cortex V4	V4C	13947362	89.50%
398-22R	ypa398	6	Female	7.7	Visual cortex V4	V4C	16390643	87.65%
398-23L	ypa398	6	Female	6.9	Superior frontal gyrus	SFG	16670565	84.70%
398-23R	ypa398	6	Female	7.7	Superior frontal gyrus	SFG	13737715	88.08%
398-24L	ypa398	6	Female	8.3	Caudate nucleus	CN	14634897	87.09%
398-24R	ypa398	6	Female	8.3	Caudate nucleus	CN	13478803	85.29%
398-25L	ypa398	6	Female	7.4	Putamen	PTM	14244948	86.05%
398-25R	ypa398	6	Female	7.7	Putamen	PTM	14534351	84.75%
398-26L	ypa398	6	Female	7.1	Global pallidum	GP	14338482	85.19%
398-26R	ypa398	6	Female	6.4	Global pallidum	GP	14749865	85.41%
398-27L	ypa398	6	Female	7.5	Amygdala	AMY	17858240	85.85%
398-27R	ypa398	6	Female	8.2	Amygdala	AMY	15489806	85.99%
398-28L	ypa398	6	Female	8.3	Hippocampus	HIP	17498181	86.83%

398-28R	ypa398	6	Female	7.7	Hippocampus	HIP	16129057	72.42%
398-2L	ypa398	6	Female	6.4	Ventral lateral prefrontal cortex	VLPFC	14223639	86.35%
398-2R	ypa398	6	Female	7.3	Ventral lateral prefrontal cortex	VLPFC	14050497	84.70%
398-31L	ypa398	6	Female	6.7	Cingulate sulcus	CGS	15422807	87.35%
398-31R	ypa398	6	Female	8	Cingulate sulcus	CGS	16005876	87.27%
398-32	ypa398	6	Female	7.2	Thalamus	TH	12684148	86.39%
398-33	ypa398	6	Female	7.9	Hypothalamus	HTH	13629825	86.10%
398-34L	ypa398	6	Female	6.3	Superior colliculus	SC	15365245	85.86%
398-34R	ypa398	6	Female	7.7	Superior colliculus	SC	16298023	88.16%
398-35L	ypa398	6	Female	7.1	Inferior colliculus	IC	12303541	84.37%
398-35R	ypa398	6	Female	8.1	Inferior colliculus	IC	14678677	85.96%
398-37	ypa398	6	Female	8.2	pons	pons	13960167	84.91%
398-38L-2	ypa398	6	Female	7.9	Cerebellar cortex	CBC	13838159	77.38%
398-38R	ypa398	6	Female	8.3	Cerebellar cortex	CBC	12512106	86.62%
398-39	ypa398	6	Female	7.5	Cerebellar vermis	CV	13007229	88.19%
398-3L	ypa398	6	Female	6.5	Anterior supraprincipal dimple	ASPD	15281926	85.75%
398-3R	ypa398	6	Female	7.7	Anterior supraprincipal dimple	ASPD	14463218	87.84%
398-40	ypa398	6	Female	7.6	Pineal gland	PG	15957711	91.17%
398-41	ypa398	6	Female	8.1	Hypophysis	HYP	15703342	88.05%
398-42L	ypa398	6	Female	7.3	Ventromedial prefrontal cortex	VMPFC	16247710	86.65%
398-42R	ypa398	6	Female	7.6	Ventromedial prefrontal cortex	VMPFC	15311298	88.68%
398-43L	ypa398	6	Female	7.4	Anterior insula cortex	AIC	13567135	84.69%
398-43R	ypa398	6	Female	7.4	Anterior insula cortex	AIC	17672804	89.18%
398-44L	ypa398	6	Female	7.8	Posterior insula cortex	PIC	13936615	70.37%
398-44R	ypa398	6	Female	7.1	Posterior insula cortex	PIC	15818854	87.49%
398-45L	ypa398	6	Female	7.8	Orbitofrontal cortex	OFC	14068929	85.41%
398-45R	ypa398	6	Female	6.7	Orbitofrontal cortex	OFC	13480517	87.68%
398-46L	ypa398	6	Female	7.3	Accumbens nucleus	ACB	12567816	84.12%
398-46R	ypa398	6	Female	7.5	Accumbens nucleus	ACB	15361933	85.71%
398-47L	ypa398	6	Female	7.9	Corpus callosum	CC	15181112	88.97%
398-47R	ypa398	6	Female	8.6	Corpus callosum	CC	16162423	86.97%
398-48R	ypa398	6	Female	7.7	Ventral tegmental area	VTA	15026628	86.04%
398-49L	ypa398	6	Female	7.3	Olfactory bulb	OB	16335593	88.25%
398-49R	ypa398	6	Female	6.9	Olfactory bulb	OB	15981334	87.89%
398-4L	ypa398	6	Female	6.4	Posterior supraprincipal dimple	PSPD	18505190	88.57%
398-4R	ypa398	6	Female	7.2	Posterior supraprincipal dimple	PSPD	14094779	86.89%
398-53	ypa398	6	Female	7.2	Medulla	MED	14302834	88.16%
398-5L	ypa398	6	Female	6.6	Superior arcuate sulcus	SAR	15451994	87.10%
398-5R	ypa398	6	Female	7.5	Superior arcuate sulcus	SAR	14855589	87.73%
398-6L	ypa398	6	Female	7.4	Principal sulcus	PS	15110209	86.68%
398-6R	ypa398	6	Female	7.5	Principal sulcus	PS	15460314	87.09%
398-7L	ypa398	6	Female	7.9	Anterior subcentral dimple	ASD	17476153	86.03%
398-7R	ypa398	6	Female	6.5	Anterior subcentral dimple	ASD	14211245	87.59%
398-8L	ypa398	6	Female	7.5	Arcuate sulcus spur	ARSP	17701214	86.51%
398-8R	ypa398	6	Female	6.6	Arcuate sulcus spur	ARSP	14568933	87.11%
398-9L-2	ypa398	6	Female	7.9	Superior precentral dimple	SPCD	16480937	91.14%
398-9R	ypa398	6	Female	7	Superior precentral dimple	SPCD	16936101	86.96%
399-10L	ypa399	5	Male	7.2	Superior postcentral dimple	SU	14013152	87.88%
399-10R	ypa399	5	Male	7.5	Superior postcentral dimple	SU	16602959	89.75%
399-11L	ypa399	5	Male	6.5	Intraparietal sulcus	IPS	17001855	87.45%
399-11R	ypa399	5	Male	7.5	Intraparietal sulcus	IPS	14414903	89.06%
399-12L	ypa399	5	Male	6.1	Lateral fissure	LF	18059909	86.81%
399-12R	ypa399	5	Male	7.2	Lateral fissure	LF	22786385	88.24%
399-13L	ypa399	5	Male	6.8	Parietal area	PEC	15327657	87.55%
399-13R	ypa399	5	Male	8.3	Parietal area	PEC	38304152	88.71%
399-14L	ypa399	5	Male	7.1	Anterior marginal gyrus	AMG	14986472	89.18%
399-14R	ypa399	5	Male	8.4	Anterior marginal gyrus	AMG	13701776	89.27%
399-15L	ypa399	5	Male	7.5	Angular gyrus	AG	16617039	87.89%
399-15R	ypa399	5	Male	7.8	Angular gyrus	AG	27642754	88.29%
399-16L	ypa399	5	Male	8.5	Lateral superior temporal gyrus	LSTG	14826750	89.57%
399-16R	ypa399	5	Male	8.1	Lateral superior temporal gyrus	LSTG	25974649	88.38%
399-17L	ypa399	5	Male	7.6	Lateral superior temporal gyrus	LSTG	15557430	88.40%
399-17R	ypa399	5	Male	8.6	Lateral superior temporal gyrus	LSTG	15877261	90.15%
399-18L	ypa399	5	Male	7.8	Temporal polar gyrus	TPG	18821134	89.06%
399-18R	ypa399	5	Male	8.4	Temporal polar gyrus	TPG	12619009	89.71%
399-19L	ypa399	5	Male	7.9	Temporal polar gyrus	TPG	14728417	89.58%
399-19R	ypa399	5	Male	7.9	Temporal polar gyrus	TPG	13458307	89.32%
399-1L	ypa399	5	Male	8	Dorsolateral prefrontal cortex	DLPFC	19071954	86.07%
399-1R	ypa399	5	Male	7.6	Dorsolateral prefrontal cortex	DLPFC	12205799	84.49%
399-20L	ypa399	5	Male	6.7	Primary visual cortex	V1C	13617955	88.25%
399-20R	ypa399	5	Male	7.7	Primary visual cortex	V1C	12669142	89.39%
399-21L	ypa399	5	Male	7.8	Visual cortex V2	V2C	12532348	78.53%
399-21R	ypa399	5	Male	8	Visual cortex V2	V2C	16175102	87.78%
399-22L	ypa399	5	Male	7.2	Visual cortex V4	V4C	21522957	89.49%
399-22R	ypa399	5	Male	7	Visual cortex V4	V4C	15014364	88.91%
399-23L	ypa399	5	Male	7.2	Superior frontal gyrus	SFG	16739927	84.05%
399-23R	ypa399	5	Male	7.5	Superior frontal gyrus	SFG	15283980	84.55%
399-24L	ypa399	5	Male	8.2	Caudate nucleus	CN	12158057	80.29%
399-24R	ypa399	5	Male	7.7	Caudate nucleus	CN	14497301	87.73%
399-25L	ypa399	5	Male	7.6	Putamen	PTM	14782501	87.84%
399-25R	ypa399	5	Male	8.6	Putamen	PTM	16208100	86.48%
399-26L	ypa399	5	Male	7.8	Global pallidum	GP	28052354	86.25%
399-26R	ypa399	5	Male	7.6	Global pallidum	GP	15115912	86.55%
399-27L	ypa399	5	Male	7.7	Amygdala	AMY	13524285	85.01%
399-27R	ypa399	5	Male	8	Amygdala	AMY	15115379	87.75%
399-28L	ypa399	5	Male	8.2	Hippocampus	HIP	17755477	89.01%
399-28R	ypa399	5	Male	8.7	Hippocampus	HIP	17673101	89.15%
399-2R	ypa399	5	Male	7.4	Ventral lateral prefrontal cortex	VLPFC	18061183	85.57%
399-31L	ypa399	5	Male	7.8	Cingulate sulcus	CGS	13919582	89.75%
399-31R	ypa399	5	Male	7.7	Cingulate sulcus	CGS	14268939	87.38%
399-32	ypa399	5	Male	7.7	Thalamus	TH	18347062	87.68%
399-33	ypa399	5	Male	8	Hypothalamus	HTH	18833311	88.59%
399-34L	ypa399	5	Male	8.4	Superior colliculus	SC	17138935	90.12%
399-34R	ypa399	5	Male	7.5	Superior colliculus	SC	16262874	86.45%
399-35L	ypa399	5	Male	7.8	Inferior colliculus	IC	18708234	86.47%
399-35R	ypa399	5	Male	7.3	Inferior colliculus	IC	20465194	88.00%
399-37	ypa399	5	Male	7.9	pons	pons	13867054	87.58%
399-38L	ypa399	5	Male	7.1	Cerebellar cortex	CBC	12735589	80.35%
399-38R	ypa399	5	Male	8.5	Cerebellar cortex	CBC	16650774	90.71%
399-39	ypa399	5	Male	8.8	Cerebellar vermis	CV	13641656	89.36%
399-3L	ypa399	5	Male	8.2	Anterior supraprincipal dimple	ASPD	14740245	86.08%
399-3R	ypa399	5	Male	7.7	Anterior supraprincipal dimple	ASPD	13205914	85.66%
399-40	ypa399	5	Male	8.6	Pineal gland	PG	21821369	90.78%
399-41	ypa399	5	Male	8.6	Hypophysis	HYP	16285271	90.68%
399-42L	ypa399	5	Male	8.2	Ventromedial prefrontal cortex	VMPFC	17811705	87.24%

399-42R	ypa399	5	Male	8.3	Ventromedial prefrontal cortex	VMPFC	17707195	87.66%
399-43L	ypa399	5	Male	8	Anterior insula cortex	AIC	13101435	86.42%
399-43R	ypa399	5	Male	8.5	Anterior insula cortex	AIC	16691738	86.47%
399-44L	ypa399	5	Male	7.9	Posterior insula cortex	PIC	18151643	86.59%
399-44R	ypa399	5	Male	7.9	Posterior insula cortex	PIC	15198910	85.31%
399-45L	ypa399	5	Male	7.2	Orbitofrontal cortex	OFC	22356138	85.26%
399-45R	ypa399	5	Male	6.4	Orbitofrontal cortex	OFC	14232659	86.43%
399-46L	ypa399	5	Male	7.7	Accumbens nucleus	ACB	13619555	86.87%
399-46R	ypa399	5	Male	8.2	Accumbens nucleus	ACB	14770197	86.63%
399-47L	ypa399	5	Male	9	Corpus callosum	CC	13851699	90.24%
399-47R	ypa399	5	Male	8.6	Corpus callosum	CC	14589665	90.41%
399-48	ypa399	5	Male	7.7	Ventral tegmental area	VTA	15395016	88.81%
399-49L	ypa399	5	Male	7.9	Olfactory bulb	OB	41216899	89.08%
399-49R	ypa399	5	Male	8.2	Olfactory bulb	OB	16306349	90.33%
399-4L	ypa399	5	Male	8.1	Posterior supraprincipal dimple	PSPD	13767523	86.33%
399-4R	ypa399	5	Male	7.3	Posterior supraprincipal dimple	PSPD	13562979	86.45%
399-53	ypa399	5	Male	7.3	Medulla	MED	30748767	85.35%
399-5L	ypa399	5	Male	6.8	Superior arcuate sulcus	SAR	16880739	85.65%
399-5R	ypa399	5	Male	7.8	Superior arcuate sulcus	SAR	14824862	86.59%
399-6L	ypa399	5	Male	7.4	Principal sulcus	PS	15581196	85.58%
399-6R	ypa399	5	Male	8.1	Principal sulcus	PS	17354811	87.29%
399-7L	ypa399	5	Male	6.8	Anterior subcentral dimple	ASD	14923392	85.30%
399-7R	ypa399	5	Male	6.8	Anterior subcentral dimple	ASD	14334775	87.04%
399-8L	ypa399	5	Male	7.1	Arcuate sulcus spur	ARSP	15193261	85.54%
399-8R	ypa399	5	Male	8.2	Arcuate sulcus spur	ARSP	14216173	88.46%
399-9L	ypa399	5	Male	6.4	Superior precentral dimple	SPCD	14853507	85.48%
399-9R	ypa399	5	Male	7.6	Superior precentral dimple	SPCD	31201918	88.32%
ypa405-10-L	ypa405	24	Female	8.1	Superior postcentral dimple	SU	14883734	91.12%
ypa405-10-R	ypa405	24	Female	8.2	Superior postcentral dimple	SU	13588868	91.12%
ypa405-11-L	ypa405	24	Female	8	Intraparietal sulcus	IPS	15724485	89.07%
ypa405-11-R	ypa405	24	Female	7.9	Intraparietal sulcus	IPS	19135408	88.32%
ypa405-12-L	ypa405	24	Female	8.2	Lateral fissure	LF	13547351	90.68%
ypa405-12-R	ypa405	24	Female	7.9	Lateral fissure	LF	25354187	90.39%
ypa405-13-L	ypa405	24	Female	8.2	Parietal area	PEC	22907580	91.04%
ypa405-13-R	ypa405	24	Female	7.2	Parietal area	PEC	15733557	91.36%
ypa405-14-L	ypa405	24	Female	8.3	Anterior marginal gyrus	AMG	13963112	91.52%
ypa405-14-R	ypa405	24	Female	8	Anterior marginal gyrus	AMG	21326100	88.57%
ypa405-15-L	ypa405	24	Female	8.3	Angular gyrus	AG	16405432	91.11%
ypa405-15-R	ypa405	24	Female	8.4	Angular gyrus	AG	11285453	71.97%
ypa405-16-L	ypa405	24	Female	8.8	Lateral superior temporal gyrus	LSTG	14349923	91.21%
ypa405-16-R	ypa405	24	Female	9.1	Lateral superior temporal gyrus	LSTG	11447603	72.08%
ypa405-17-L	ypa405	24	Female	8.4	Lateral superior temporal gyrus	LSTG	16280718	90.20%
ypa405-17-R-2	ypa405	24	Female	8.7	Lateral superior temporal gyrus	LSTG	18350575	89.33%
ypa405-18-L	ypa405	24	Female	8.4	Temporal polar gyrus	TPG	14850304	91.14%
ypa405-18-R	ypa405	24	Female	8.3	Temporal polar gyrus	TPG	11457914	73.94%
ypa405-19-L	ypa405	24	Female	7.9	Temporal polar gyrus	TPG	19166636	90.71%
ypa405-19-R	ypa405	24	Female	8	Temporal polar gyrus	TPG	11456799	74.71%
ypa405-1-L	ypa405	24	Female	7.5	Dorsolateral prefrontal cortex	DLPFC	18080513	90.80%
ypa405-1-R	ypa405	24	Female	8.3	Dorsolateral prefrontal cortex	DLPFC	14131362	91.30%
ypa405-20-L	ypa405	24	Female	8.1	Primary visual cortex	V1C	15807591	90.67%
ypa405-20-R	ypa405	24	Female	7.7	Primary visual cortex	V1C	11953401	74.01%
ypa405-21-L	ypa405	24	Female	7.3	Visual cortex V2	V2C	19564731	90.50%
ypa405-21-R	ypa405	24	Female	8.5	Visual cortex V2	V2C	13410007	73.18%
ypa405-22-L	ypa405	24	Female	7.8	Visual cortex V4	V4C	13768312	91.56%
ypa405-22-R	ypa405	24	Female	6.6	Visual cortex V4	V4C	12510483	71.80%
ypa405-23-L	ypa405	24	Female	8.3	Superior frontal gyrus	SFG	16598686	90.15%
ypa405-23-R	ypa405	24	Female	8.6	Superior frontal gyrus	SFG	13578244	90.97%
ypa405-24-L	ypa405	24	Female	8.5	Caudate nucleus	CN	16364424	89.78%
ypa405-24-R	ypa405	24	Female	8.1	Caudate nucleus	CN	13414786	70.39%
ypa405-25-L	ypa405	24	Female	9.1	Putamen	PTM	13374906	89.73%
ypa405-25-R	ypa405	24	Female	8.3	Putamen	PTM	11941045	68.52%
ypa405-26-L	ypa405	24	Female	8	Global pallidum	GP	14699286	89.79%
ypa405-26-R	ypa405	24	Female	7.6	Global pallidum	GP	14756932	89.09%
ypa405-27-L	ypa405	24	Female	8.7	Amygdala	AMY	20687646	90.69%
ypa405-27-R	ypa405	24	Female	8.5	Amygdala	AMY	12931461	70.96%
ypa405-28-L	ypa405	24	Female	8.7	Hippocampus	HIP	14129995	91.07%
ypa405-28-R	ypa405	24	Female	8.3	Hippocampus	HIP	12479081	74.72%
ypa405-2-L	ypa405	24	Female	8.3	Ventral lateral prefrontal cortex	VLPFC	14067637	90.26%
ypa405-2-R	ypa405	24	Female	8.6	Ventral lateral prefrontal cortex	VLPFC	15415872	89.79%
ypa405-31-L	ypa405	24	Female	8.8	Cingulate sulcus	CGS	17433921	91.51%
ypa405-31-R	ypa405	24	Female	8.4	Cingulate sulcus	CGS	18882776	90.06%
ypa405-32-L	ypa405	24	Female	7.9	Thalamus	TH	16030419	89.79%
ypa405-33-L	ypa405	24	Female	8.6	Hypothalamus	HTH	14409142	90.35%
ypa405-34-L	ypa405	24	Female	8.4	Superior colliculus	SC	14714687	91.48%
ypa405-34-R	ypa405	24	Female	8.2	Superior colliculus	SC	15667633	91.98%
ypa405-35-L	ypa405	24	Female	7.5	Inferior colliculus	IC	24600247	89.39%
ypa405-35-R	ypa405	24	Female	8.3	Inferior colliculus	IC	15218819	91.10%
ypa405-37-L-2	ypa405	24	Female	8.7	pons	pons	15574493	88.79%
ypa405-38-L	ypa405	24	Female	8.6	Cerebellar cortex	CBC	22431726	91.66%
ypa405-38-R	ypa405	24	Female	9.2	Cerebellar cortex	CBC	29946238	92.27%
ypa405-39-L	ypa405	24	Female	9	Cerebellar vermis	CV	15154488	91.63%
ypa405-3-L	ypa405	24	Female	8.9	Anterior supraprincipal dimple	ASPD	15125560	88.08%
ypa405-3-R	ypa405	24	Female	8.4	Anterior supraprincipal dimple	ASPD	15867162	89.89%
ypa405-40_R	ypa405	24	Female	7.1	Pineal gland	PG	13873212	93.78%
ypa405-41_R	ypa405	24	Female	7.1	Hypophysis	HYP	14503772	92.86%
ypa405-42-L	ypa405	24	Female	8.4	Ventromedial prefrontal cortex	VMPFC	22680180	91.37%
ypa405-42-R	ypa405	24	Female	7.9	Ventromedial prefrontal cortex	VMPFC	15681592	89.57%
ypa405-43-L	ypa405	24	Female	8.4	Anterior insula cortex	AIC	17812359	90.35%
ypa405-43-R	ypa405	24	Female	9.1	Anterior insula cortex	AIC	21834064	90.21%
ypa405-44-L	ypa405	24	Female	8.6	Posterior insula cortex	PIC	16370074	91.30%
ypa405-45-L	ypa405	24	Female	8.5	Orbitofrontal cortex	OFC	15586744	90.31%
ypa405-45-R	ypa405	24	Female	8.3	Orbitofrontal cortex	OFC	17688690	88.68%
ypa405-46-L	ypa405	24	Female	8.6	Accumbens nucleus	ACB	18206906	90.03%
ypa405-46-R	ypa405	24	Female	8.5	Accumbens nucleus	ACB	12723373	73.14%
ypa405-47-L	ypa405	24	Female	8.8	Corpus callosum	CC	14930638	91.00%
ypa405-47-R	ypa405	24	Female	8	Corpus callosum	CC	15870685	92.01%
ypa405-49-L	ypa405	24	Female	8.9	Olfactory bulb	OB	17631264	90.83%
ypa405-49-R	ypa405	24	Female	9.1	Olfactory bulb	OB	20796789	92.28%
ypa405-4-L	ypa405	24	Female	8.5	Posterior supraprincipal dimple	PSPD	20691665	90.27%
ypa405-4-R	ypa405	24	Female	8.6	Posterior supraprincipal dimple	PSPD	17722468	88.91%
ypa405-53_R	ypa405	24	Female	7.1	Medulla	MED	18425386	90.02%
ypa405-5-L	ypa405	24	Female	7.8	Superior arcuate sulcus	SAR	20258443	89.64%
ypa405-5-R	ypa405	24	Female	8.5	Superior arcuate sulcus	SAR	13789070	90.38%
ypa405-6-L	ypa405	24	Female	8.3	Principal sulcus	PS	21872602	91.75%
ypa405-6-R	ypa405	24	Female	8.7	Principal sulcus	PS	12736991	88.62%

ypa405-7-L	ypa405	24	Female	8.2	Anterior subcentral dimple	ASD	14136261	90.43%
ypa405-7-R	ypa405	24	Female	8.5	Anterior subcentral dimple	ASD	22657448	88.93%
ypa405-8-L	ypa405	24	Female	7.6	Arcuate sulcus spur	ARSP	35507337	90.79%
ypa405-8-R	ypa405	24	Female	8.3	Arcuate sulcus spur	ARSP	15098610	87.40%
ypa405-9-L	ypa405	24	Female	8.1	Superior precentral dimple	SPCD	14422433	91.36%
ypa405-9-R	ypa405	24	Female	8.3	Superior precentral dimple	SPCD	23274905	90.10%
ypa406-10-L	ypa406	16	Female	8	Superior postcentral dimple	SU	16066465	88.91%
ypa406-10-R	ypa406	16	Female	8	Superior postcentral dimple	SU	15997421	89.23%
ypa406-11-L	ypa406	16	Female	8.2	Intraparietal sulcus	IPS	16044571	91.16%
ypa406-11-R	ypa406	16	Female	8.1	Intraparietal sulcus	IPS	13716151	89.48%
ypa406-12-L	ypa406	16	Female	8.5	Lateral fissure	LF	29492898	90.06%
ypa406-12-R	ypa406	16	Female	8.3	Lateral fissure	LF	13099556	88.89%
ypa406-13-L	ypa406	16	Female	7.9	Parietal area	PEC	18792968	91.93%
ypa406-13-R	ypa406	16	Female	8	Parietal area	PEC	14758609	90.39%
ypa406-14-L	ypa406	16	Female	7.3	Anterior marginal gyrus	AMG	16159365	91.53%
ypa406-14-R	ypa406	16	Female	8.1	Anterior marginal gyrus	AMG	30423096	90.49%
ypa406-15-L	ypa406	16	Female	7.7	Angular gyrus	AG	17345058	88.28%
ypa406-15-R	ypa406	16	Female	8	Angular gyrus	AG	14731768	90.06%
ypa406-16-L-2	ypa406	16	Female	7.9	Lateral superior temporal gyrus	LSTG	14496089	89.61%
ypa406-16-R	ypa406	16	Female	8	Lateral superior temporal gyrus	LSTG	15577274	90.42%
ypa406-17-L	ypa406	16	Female	8	Lateral superior temporal gyrus	LSTG	34409713	91.02%
ypa406-17-R	ypa406	16	Female	7.3	Lateral superior temporal gyrus	LSTG	27543506	89.37%
ypa406-18-L	ypa406	16	Female	7.7	Temporal polar gyrus	TPG	13621541	90.66%
ypa406-18-R	ypa406	16	Female	7.8	Temporal polar gyrus	TPG	13125521	90.97%
ypa406-19-L	ypa406	16	Female	7.9	Temporal polar gyrus	TPG	23410070	92.00%
ypa406-19-R	ypa406	16	Female	7.7	Temporal polar gyrus	TPG	18098207	90.01%
ypa406-1-L	ypa406	16	Female	7.6	Dorsolateral prefrontal cortex	DLPFC	26933279	91.25%
ypa406-1-R	ypa406	16	Female	6.4	Dorsolateral prefrontal cortex	DLPFC	13977506	86.45%
ypa406-20-L	ypa406	16	Female	7	Primary visual cortex	V1C	25304428	90.58%
ypa406-20-R	ypa406	16	Female	7.5	Primary visual cortex	V1C	16478676	90.55%
ypa406-21-L	ypa406	16	Female	7.3	Visual cortex V2	V2C	17872786	90.93%
ypa406-21-R	ypa406	16	Female	7.1	Visual cortex V2	V2C	27631039	89.83%
ypa406-22-L	ypa406	16	Female	7.8	Visual cortex V4	V4C	18955267	91.33%
ypa406-22-R	ypa406	16	Female	6.3	Visual cortex V4	V4C	21199308	91.38%
ypa406-23-L	ypa406	16	Female	8.1	Superior frontal gyrus	SFG	14962799	90.84%
ypa406-23-R	ypa406	16	Female	6.2	Superior frontal gyrus	SFG	32173321	88.42%
ypa406-24-L	ypa406	16	Female	7.9	Caudate nucleus	CN	20986614	87.45%
ypa406-24-R	ypa406	16	Female	8.5	Caudate nucleus	CN	18460158	88.78%
ypa406-25-L	ypa406	16	Female	8.3	Putamen	PTM	65512781	89.65%
ypa406-25-R	ypa406	16	Female	7.9	Putamen	PTM	18332725	87.98%
ypa406-26-L	ypa406	16	Female	7.9	Global pallidum	GP	13933883	89.36%
ypa406-26-R	ypa406	16	Female	8.1	Global pallidum	GP	13653117	90.10%
ypa406-27-L	ypa406	16	Female	7.8	Amygdala	AMY	15295672	90.31%
ypa406-27-R	ypa406	16	Female	8.3	Amygdala	AMY	13512127	90.71%
ypa406-28-L	ypa406	16	Female	8	Hippocampus	HIP	27235279	88.69%
ypa406-28-R	ypa406	16	Female	7.6	Hippocampus	HIP	15202508	87.56%
ypa406-2-L	ypa406	16	Female	8	Ventral lateral prefrontal cortex	VLPFC	14345678	88.85%
ypa406-2-R	ypa406	16	Female	8.1	Ventral lateral prefrontal cortex	VLPFC	15527099	83.73%
ypa406-31-L	ypa406	16	Female	7.4	Cingulate sulcus	CGS	55806453	90.41%
ypa406-31-R	ypa406	16	Female	8.3	Cingulate sulcus	CGS	13133048	90.35%
ypa406-32-L	ypa406	16	Female	7.4	Thalamus	TH	15097713	89.65%
ypa406-33-L	ypa406	16	Female	7.7	Hypothalamus	HTH	17753521	90.51%
ypa406-34-L	ypa406	16	Female	7.7	Superior colliculus	SC	14272227	89.51%
ypa406-34-R	ypa406	16	Female	8.4	Superior colliculus	SC	13400188	91.00%
ypa406-35-L	ypa406	16	Female	8.2	Inferior colliculus	IC	72867717	86.47%
ypa406-35-R	ypa406	16	Female	7	Inferior colliculus	IC	13320482	90.30%
ypa406-37-L	ypa406	16	Female	8.1	pons	pons	16170985	85.81%
ypa406-38-L	ypa406	16	Female	8	Cerebellar cortex	CBC	19497304	91.32%
ypa406-38-R	ypa406	16	Female	7.2	Cerebellar cortex	CBC	13789616	90.70%
ypa406-39-L	ypa406	16	Female	8.1	Cerebellar vermis	CV	17614359	92.05%
ypa406-3-L	ypa406	16	Female	8.1	Anterior supraprincipal dimple	ASPD	20963901	91.47%
ypa406-3-R	ypa406	16	Female	7.8	Anterior supraprincipal dimple	ASPD	19089325	82.04%
ypa406-40_R	ypa406	16	Female	7.1	Pineal gland	PG	15539192	93.87%
ypa406-41_R	ypa406	16	Female	7.1	Hypophysis	HYP	16993932	92.10%
ypa406-42-L	ypa406	16	Female	7.9	Ventromedial prefrontal cortex	VMPFC	13976401	91.63%
ypa406-42-R	ypa406	16	Female	7.3	Ventromedial prefrontal cortex	VMPFC	21578439	86.18%
ypa406-43-L	ypa406	16	Female	7.6	Anterior insula cortex	AIC	14883076	90.91%
ypa406-43-R	ypa406	16	Female	8	Anterior insula cortex	AIC	25026627	84.56%
ypa406-44-L	ypa406	16	Female	9	Posterior insula cortex	PIC	14022202	90.88%
ypa406-45-L	ypa406	16	Female	7.3	Orbitofrontal cortex	OFC	15720654	90.22%
ypa406-45-R	ypa406	16	Female	7.5	Orbitofrontal cortex	OFC	15341327	84.61%
ypa406-46-L	ypa406	16	Female	7.3	Accumbens nucleus	ACB	51136833	86.94%
ypa406-46-R	ypa406	16	Female	7.3	Accumbens nucleus	ACB	10940585	88.94%
ypa406-47-R	ypa406	16	Female	8.9	Corpus callosum	CC	16588565	92.75%
ypa406-48-L	ypa406	16	Female	6.9	Ventral tegmental area	VTA	23057495	88.62%
ypa406-49-L	ypa406	16	Female	7.9	Olfactory bulb	OB	15544701	90.36%
ypa406-4-L	ypa406	16	Female	7.5	Posterior supraprincipal dimple	PSPD	20260643	90.51%
ypa406-4-R	ypa406	16	Female	6.9	Posterior supraprincipal dimple	PSPD	20251488	89.96%
ypa406-53	ypa406	16	Female	7.8	Medulla	MED	14480475	86.04%
ypa406-5-L	ypa406	16	Female	7.4	Superior arcuate sulcus	SAR	19654509	90.83%
ypa406-5-R	ypa406	16	Female	6.6	Superior arcuate sulcus	SAR	12681944	89.21%
ypa406-6-L	ypa406	16	Female	8	Principal sulcus	PS	15731985	91.32%
ypa406-6-R	ypa406	16	Female	8	Principal sulcus	PS	17744608	90.27%
ypa406-7-L	ypa406	16	Female	6.9	Anterior subcentral dimple	ASD	15434426	90.33%
ypa406-7-R	ypa406	16	Female	6.9	Anterior subcentral dimple	ASD	13546907	83.31%
ypa406-8-L	ypa406	16	Female	7.4	Arcuate sulcus spur	ARSP	14611697	89.15%
ypa406-8-R	ypa406	16	Female	7	Arcuate sulcus spur	ARSP	13578684	85.04%
ypa406-9-L	ypa406	16	Female	8.1	Superior precentral dimple	SPCD	14403515	90.79%
ypa406-9-R	ypa406	16	Female	7.1	Superior precentral dimple	SPCD	24046273	80.98%
ypa407-10-L	ypa407	17	Female	8	Superior postcentral dimple	SU	14196759	90.09%
ypa407-10-R	ypa407	17	Female	7.4	Superior postcentral dimple	SU	15111885	89.29%
ypa407-11-L	ypa407	17	Female	7.4	Intraparietal sulcus	IPS	17004563	89.66%
ypa407-11-R	ypa407	17	Female	7.1	Intraparietal sulcus	IPS	12707328	90.04%
ypa407-12-L	ypa407	17	Female	6.7	Lateral fissure	LF	14588777	89.14%
ypa407-12-R	ypa407	17	Female	7.8	Lateral fissure	LF	13562169	87.97%
ypa407-13-L	ypa407	17	Female	7.3	Parietal area	PEC	17997093	87.47%
ypa407-13-R	ypa407	17	Female	8.3	Parietal area	PEC	18157861	90.56%
ypa407-14-L	ypa407	17	Female	8.1	Anterior marginal gyrus	AMG	11097702	88.56%
ypa407-14-R	ypa407	17	Female	6.8	Anterior marginal gyrus	AMG	13615027	89.47%
ypa407-15-L	ypa407	17	Female	7	Angular gyrus	AG	78632914	82.18%
ypa407-15-R	ypa407	17	Female	6.8	Angular gyrus	AG	29728850	89.48%
ypa407-16-L	ypa407	17	Female	8.3	Lateral superior temporal gyrus	LSTG	14173512	88.27%
ypa407-16-R	ypa407	17	Female	8.3	Lateral superior temporal gyrus	LSTG	13980742	89.95%
ypa407-17-L	ypa407	17	Female	7.8	Lateral superior temporal gyrus	LSTG	11776857	89.14%
ypa407-17-R	ypa407	17	Female	7.2	Lateral superior temporal gyrus	LSTG	21419694	88.44%

ypa407-18-L	ypa407	17	Female	8.4	Temporal polar gyrus	TPG	17241657	88.82%
ypa407-18-R	ypa407	17	Female	7	Temporal polar gyrus	TPG	31268592	89.03%
ypa407-19-L	ypa407	17	Female	6	Temporal polar gyrus	TPG	20342995	90.81%
ypa407-19-R	ypa407	17	Female	7.3	Temporal polar gyrus	TPG	16186821	56.37%
ypa407-1-L	ypa407	17	Female	8	Dorsolateral prefrontal cortex	DLPFC	14053870	90.21%
ypa407-1-R	ypa407	17	Female	7.4	Dorsolateral prefrontal cortex	DLPFC	16309501	89.47%
ypa407-20-L	ypa407	17	Female	8.3	Primary visual cortex	V1C	13367337	91.04%
ypa407-20-R	ypa407	17	Female	6.6	Primary visual cortex	V1C	17885751	90.05%
ypa407-21-L	ypa407	17	Female	7.9	Visual cortex V2	V2C	22860598	89.61%
ypa407-21-R	ypa407	17	Female	7.1	Visual cortex V2	V2C	16562647	89.75%
ypa407-22-L	ypa407	17	Female	7.4	Visual cortex V4	V4C	18972640	89.21%
ypa407-23-L	ypa407	17	Female	8.1	Superior frontal gyrus	SFG	12478196	90.06%
ypa407-23-R	ypa407	17	Female	7	Superior frontal gyrus	SFG	15102116	88.68%
ypa407-24-L	ypa407	17	Female	8.1	Caudate nucleus	CN	15806827	87.98%
ypa407-24-R	ypa407	17	Female	7	Caudate nucleus	CN	15142747	88.53%
ypa407-25-L	ypa407	17	Female	8.2	Putamen	PTM	16080282	87.32%
ypa407-25-R	ypa407	17	Female	8.1	Putamen	PTM	16624318	89.46%
ypa407-26-L	ypa407	17	Female	7.7	Global pallidum	GP	20297211	88.47%
ypa407-26-R	ypa407	17	Female	7.6	Global pallidum	GP	14635592	87.68%
ypa407-27-L	ypa407	17	Female	7.2	Amygdala	AMY	13768717	88.03%
ypa407-27-R	ypa407	17	Female	8.2	Amygdala	AMY	20546724	90.06%
ypa407-28-L	ypa407	17	Female	6.6	Hippocampus	HIP	14724568	87.17%
ypa407-28-R	ypa407	17	Female	8.1	Hippocampus	HIP	14834926	89.74%
ypa407-2-L	ypa407	17	Female	7.6	Ventral lateral prefrontal cortex	VLPFC	15766591	89.13%
ypa407-2-R	ypa407	17	Female	6.2	Ventral lateral prefrontal cortex	VLPFC	12653115	87.90%
ypa407-31-L	ypa407	17	Female	6	Cingulate sulcus	CGS	16968439	89.69%
ypa407-31-R	ypa407	17	Female	7.3	Cingulate sulcus	CGS	13257428	89.98%
ypa407-32-L	ypa407	17	Female	4.8	Thalamus	TH	18079650	89.16%
ypa407-33-L	ypa407	17	Female	7	Hypothalamus	HTH	14099806	89.05%
ypa407-34-L	ypa407	17	Female	5.6	Superior colliculus	SC	17965729	91.29%
ypa407-34-R	ypa407	17	Female	8.1	Superior colliculus	SC	14720464	90.04%
ypa407-35-L	ypa407	17	Female	7	Inferior colliculus	IC	12732659	89.33%
ypa407-35-R	ypa407	17	Female	7.4	Inferior colliculus	IC	13025541	88.90%
ypa407-37-L	ypa407	17	Female	7.3	pons	pons	15687948	88.23%
ypa407-38-L	ypa407	17	Female	8.8	Cerebellar cortex	CBC	15782934	91.53%
ypa407-38-R	ypa407	17	Female	8.4	Cerebellar cortex	CBC	15574488	92.25%
ypa407-39-L	ypa407	17	Female	8.3	Cerebellar vermis	CV	15081637	91.67%
ypa407-3-L	ypa407	17	Female	6.9	Anterior supraprincipal dimple	ASPD	13771025	89.73%
ypa407-3-R	ypa407	17	Female	7.9	Anterior supraprincipal dimple	ASPD	15031177	89.91%
ypa407-40_R	ypa407	17	Female	7.1	Pineal gland	PG	15802820	93.51%
ypa407-41_R	ypa407	17	Female	7.1	Hypophysis	HYP	14017755	92.09%
ypa407-42-L	ypa407	17	Female	8.6	Ventromedial prefrontal cortex	VMPFC	13286436	90.29%
ypa407-42-R	ypa407	17	Female	8.2	Ventromedial prefrontal cortex	VMPFC	14475328	89.55%
ypa407-43-L	ypa407	17	Female	8.2	Anterior insula cortex	AIC	13575752	89.81%
ypa407-43-R	ypa407	17	Female	8.3	Anterior insula cortex	AIC	14103497	88.32%
ypa407-44-L	ypa407	17	Female	7.6	Posterior insula cortex	PIC	15473888	91.11%
ypa407-44-R	ypa407	17	Female	8.1	Posterior insula cortex	PIC	15819118	89.17%
ypa407-45-L	ypa407	17	Female	7.2	Orbitofrontal cortex	OFC	13483070	89.58%
ypa407-45-R	ypa407	17	Female	7.3	Orbitofrontal cortex	OFC	12816779	89.67%
ypa407-46-L	ypa407	17	Female	7.7	Accumbens nucleus	ACB	14432260	87.47%
ypa407-46-R	ypa407	17	Female	8.1	Accumbens nucleus	ACB	13737307	87.29%
ypa407-47-L	ypa407	17	Female	7.9	Corpus callosum	CC	18560843	92.38%
ypa407-47-R	ypa407	17	Female	8.5	Corpus callosum	CC	12909287	93.20%
ypa407-48-L	ypa407	17	Female	7.1	Ventral tegmental area	VTA	12845819	88.87%
ypa407-4-L	ypa407	17	Female	7.4	Posterior supraprincipal dimple	PSPD	16274044	88.09%
ypa407-4-R	ypa407	17	Female	6.5	Posterior supraprincipal dimple	PSPD	13834845	88.13%
ypa407-53	ypa407	17	Female	7.1	Medulla	MED	15534960	90.33%
ypa407-5-L	ypa407	17	Female	7.8	Superior arcuate sulcus	SAR	12710641	90.26%
ypa407-5-R	ypa407	17	Female	7.1	Superior arcuate sulcus	SAR	12711247	88.86%
ypa407-6-L	ypa407	17	Female	7.7	Principal sulcus	PS	15146629	90.23%
ypa407-6-R	ypa407	17	Female	7.8	Principal sulcus	PS	14374486	89.67%
ypa407-7-L	ypa407	17	Female	7.6	Anterior subcentral dimple	ASD	11289419	88.64%
ypa407-7-R	ypa407	17	Female	5.7	Anterior subcentral dimple	ASD	21527288	90.40%
ypa407-8-L	ypa407	17	Female	7.6	Arcuate sulcus spur	ARSP	12275953	89.19%
ypa407-8-R	ypa407	17	Female	7	Arcuate sulcus spur	ARSP	13281625	86.65%
ypa407-9-L	ypa407	17	Female	8	Superior precentral dimple	SPCD	13338481	90.12%
ypa407-9-R	ypa407	17	Female	7.3	Superior precentral dimple	SPCD	15271269	88.15%

AMY

Lineages \ Development windows	w2	w3	w4	w5	w6	w7	w8	w9
Homo sapiens	46.20522	45.63062	46.28162	52.52151	54.97806	53.60063	51.29821	53.50605
Hominini	35.5124	36.89676	36.74298	41.3953	41.80997	40.56427	40.88987	42.20634
Hominninae	29.92812	29.27995	27.97513	35.05604	37.50938	35.2342	32.42862	35.44774
Hominidae	46.2285	46.26543	47.09032	57.78443	58.3479	56.55745	55.52057	56.28701
Hominoidea	28.89687	28.83581	29.84042	36.38534	37.00535	36.2547	34.42595	36.30717
Catarrhini	23.18839	22.74999	23.01007	27.54859	28.77981	26.8161	25.49529	26.0044
Simiiformes	6.14303	6.176696	5.966764	5.586742	5.387054	6.16752	6.241788	5.90765
Haplorrhini	46.93007	47.02942	47.16963	50.26871	52.39051	52.19534	53.22792	54.83741

STR

Lineages \ Development windows	w2	w3	w4	w5	w6	w7	w8	w9
Homo sapiens	47.07729	46.8012	47.22401	54.55073	56.96182	55.85488	54.31063	55.38351
Hominini	37.11685	36.3927	37.73633	42.82705	43.43578	42.16453	43.64754	44.61677
Hominninae	31.1269	29.27323	30.06505	38.93008	40.77757	43.60597	39.66646	40.95462
Hominidae	46.7017	46.0248	48.12021	57.93416	59.20873	57.92935	55.61361	57.94253
Hominoidea	28.70765	28.75027	29.23832	37.37386	38.17435	38.81252	37.40978	38.09747
Catarrhini	24.5608	24.48883	25.25615	30.68546	31.29368	33.29257	29.1934	28.05865
Simiiformes	8.791691	8.045679	8.06525	5.286706	4.977894	5.831445	5.257429	5.276077
Haplorrhini	49.23112	50.43718	50.26168	52.96354	55.69344	62.10617	58.23023	58.30511

HIP

Lineages \ Development windows	w2	w3	w4	w5	w6	w7	w8	w9
Homo sapiens	45.26117	49.05025	49.4307	51.3728	55.39541	53.98433	54.20618	52.19588
Hominini	35.35697	36.62382	36.57675	40.57757	41.73637	39.87661	42.41785	39.7938
Hominninae	29.68967	30.56738	27.53593	33.85399	38.12873	35.22263	36.05207	34.33535
Hominidae	47.3621	49.28135	50.1884	56.69383	58.95368	56.13545	58.43054	55.35263
Hominoidea	29.71963	32.83153	32.30543	35.99741	37.56885	36.63352	37.49305	35.00614
Catarrhini	25.49184	27.98567	28.68839	27.63202	29.97521	27.32788	26.27788	26.16601
Simiiformes	6.154078	6.487662	6.654515	5.730686	5.252576	5.562077	5.234938	5.882599
Haplorrhini	46.6258	47.72142	50.33139	48.74785	52.70611	51.80339	51.05484	53.86814

MD

Lineages \ Development windows	w2	w3	w4	w5	w6	w7	w8	w9
Homo sapiens	49.17842	49.91763	52.78924	55.14508	54.56933	53.01977	51.57261	53.35479
Hominini	36.83105	37.89695	40.13031	40.12427	39.93762	38.77825	39.15466	40.05903
Hominninae	29.10657	28.28058	29.41826	36.92311	36.4669	34.7824	34.65578	35.69952
Hominidae	47.36504	49.85115	53.48356	58.2547	58.68049	58.4373	56.38035	56.16025
Hominoidea	28.49023	30.7136	32.70236	36.56409	35.67997	35.15858	34.86177	35.46858
Catarrhini	26.42063	28.08554	29.77106	30.36385	31.03726	31.23104	29.55463	29.61672
Simiiformes	8.667097	8.900873	8.85007	6.179071	6.266805	7.399537	7.252118	6.971941
Haplorrhini	54.74853	60.0449	60.32	55.10352	58.69297	59.45526	60.01368	60.27529

NCX

Lineages \ Development windows	w2	w3	w4	w5	w6	w7	w8	w9
Homo sapiens	43.9404	45.84806	46.23798	51.54555	52.89629	53.60897	51.45694	50.38308
Hominini	33.83136	35.68159	35.98528	39.93415	39.67077	39.54965	40.99876	40.28699
Hominninae	29.60924	28.60004	28.18428	32.91083	35.23489	35.74144	33.26436	32.31757
Hominidae	44.94519	45.30242	46.04361	54.21154	56.39859	55.53543	55.91573	54.89158
Hominoidea	28.3107	27.85442	28.23373	34.13943	35.58415	36.73554	35.31749	34.0773
Catarrhini	22.62285	22.53665	23.76804	27.68321	28.14853	27.53689	26.13408	25.61506
Simiiformes	5.769789	6.124823	6.45186	6.104333	5.467227	5.660056	5.936162	6.169457
Haplorrhini	46.14329	47.80405	49.08142	50.23153	52.52921	52.76956	53.24243	55.20709

CBC

Lineages \ Development windows	w2	w3	w4	w5	w6	w7	w8	w9
Homo sapiens	45.12821	45.49736	45.54394	48.57286	48.83222	48.74015	48.94687	49.57007
Hominini	36.53739	38.00795	35.73948	38.3954	36.97753	36.3955	36.30857	36.77463
Hominninae	29.62942	33.15778	29.03912	33.00435	32.78381	31.39451	30.701	32.44449
Hominidae	45.06028	49.81105	46.48978	53.12021	54.56465	55.75396	55.51594	54.53466
Hominoidea	29.23691	32.07746	29.63529	34.18189	33.61512	33.077	32.76475	33.64966
Catarrhini	25.93124	24.21058	24.16966	26.03102	26.55365	25.44603	25.15981	26.05067
Simiiformes	7.413842	6.310459	6.156361	6.344851	6.500167	6.550869	6.320827	6.325887
Haplorrhini	48.72622	49.42686	46.76037	47.55046	50.72567	51.95239	51.54739	53.93444

Human brain areas / Lineages	HTH	PTM	ACB	CN	FC	HIP	SPC	Cerebellum	Cortex	ACC	SN	AMY
Homo sapiens	75.97254629	75.98567358	75.97150282	75.9791275	75.9760825	75.97861746	75.97177527	75.91087673	75.97112149	75.98144211	75.98105801	75.98619094

FC	Frontal cortex
ACC	Anterior cingulate cortex
AMY	Amygdala
HIP	Hippocampus
PTM	Putamen
ACB	Accumbens nucleus
CN	Caudate nucleus
HTH	Hypothalamus
SN	Substantia nigra
SPC	Spinal cord

AMY

Development windows / Lineages	w2	w3	w4	w5	w6	w7	w8	w9
Homo sapiens	76.1828	76.1809	76.1838	76.1353	76.0156	76.1551	76.114	76.1602

STR

Development windows / Lineages	w2	w3	w4	w5	w6	w7	w8	w9
Homo sapiens	76.1803	76.18	76.1819	76.1085	76.0189	76.1668	76.097	76.1543

HIP

Development windows / Lineages	w2	w3	w4	w5	w6	w7	w8	w9
Homo sapiens	76.1839	76.1834	76.1859	76.1115	76.0606	76.1614	76.1365	76.1601

MD

Development windows / Lineages	w2	w3	w4	w5	w6	w7	w8	w9
Homo sapiens	76.1745	76.1783	76.1768	76.11	76.0629	76.16	76.0767	76.1466

NCX

Development windows / Lineages	w2	w3	w4	w5	w6	w7	w8	w9
Homo sapiens	76.1722	76.1772	76.1753	76.145	76.1109	76.1619	76.1251	76.1594

CBC

Development windows / Lineages	w2	w3	w4	w5	w6	w7	w8	w9
Homo sapiens	76.1787	76.1837	76.1744	76.1552	76.1205	76.1448	76.1237	76.127